



The Consultative Committee for Space Data Systems

Report Concerning Space Data System Standards

DELTA-DOR— TECHNICAL CHARACTERISTICS AND PERFORMANCE

INFORMATIONAL REPORT

CCSDS 500.1-G-2

GREEN BOOK

November 2019

Report Concerning Space Data System Standards

**DELTA-DOR—
TECHNICAL
CHARACTERISTICS
AND PERFORMANCE**

INFORMATIONAL REPORT

CCSDS 500.1-G-2

GREEN BOOK

November 2019

AUTHORITY

Issue:	Informational Report, Issue 2
Date:	November 2019
Location:	Washington, DC, USA

This document has been approved for publication by the Management Council of the Consultative Committee for Space Data Systems (CCSDS) and reflects the consensus of technical panel experts from CCSDS Member Agencies. The procedure for review and authorization of CCSDS Reports is detailed in *Organization and Processes for the Consultative Committee for Space Data Systems* (CCSDS A02.1-Y-4).

This document is published and maintained by:

CCSDS Secretariat
National Aeronautics and Space Administration
Washington, DC, USA
Email: secretariat@mailman.ccsds.org

FOREWORD

This Report contains technical material to supplement the CCSDS Recommendations for the standardization of Delta Differential One-way Ranging operations by CCSDS Member Agencies. The topics covered herein include a general description of the technique, theoretical background, definition of observables, estimates of system performance, system trade-offs, and descriptions of existing systems. This Report deals explicitly with the technical definitions and conventions associated with inter-Agency cross-support situations involving Delta Differential One-way Ranging operations.

Through the process of normal evolution, it is expected that expansion, deletion, or modification of this document may occur. This Report is therefore subject to CCSDS document management and change control procedures, which are defined in *Organization and Processes for the Consultative Committee for Space Data Systems* (CCSDS A02.1-Y-4). Current versions of CCSDS documents are maintained at the CCSDS Web site:

<http://www.ccsds.org/>

Questions relating to the contents or status of this document should be sent to the CCSDS Secretariat at the email address indicated on page i.

CCSDS REPORT CONCERNING DELTA-DOR—
TECHNICAL CHARACTERISTICS AND PERFORMANCE

At time of publication, the active Member and Observer Agencies of the CCSDS were:

Member Agencies

- Agenzia Spaziale Italiana (ASI)/Italy.
- Canadian Space Agency (CSA)/Canada.
- Centre National d'Etudes Spatiales (CNES)/France.
- China National Space Administration (CNSA)/People's Republic of China.
- Deutsches Zentrum für Luft- und Raumfahrt (DLR)/Germany.
- European Space Agency (ESA)/Europe.
- Federal Space Agency (FSA)/Russian Federation.
- Instituto Nacional de Pesquisas Espaciais (INPE)/Brazil.
- Japan Aerospace Exploration Agency (JAXA)/Japan.
- National Aeronautics and Space Administration (NASA)/USA.
- UK Space Agency/United Kingdom.

Observer Agencies

- Austrian Space Agency (ASA)/Austria.
- Belgian Federal Science Policy Office (BFSP0)/Belgium.
- Central Research Institute of Machine Building (TsNIIMash)/Russian Federation.
- China Satellite Launch and Tracking Control General, Beijing Institute of Tracking and Telecommunications Technology (CLTC/BITTT)/China.
- Chinese Academy of Sciences (CAS)/China.
- China Academy of Space Technology (CAST)/China.
- Commonwealth Scientific and Industrial Research Organization (CSIRO)/Australia.
- Danish National Space Center (DNSC)/Denmark.
- Departamento de Ciência e Tecnologia Aeroespacial (DCTA)/Brazil.
- Electronics and Telecommunications Research Institute (ETRI)/Korea.
- European Organization for the Exploitation of Meteorological Satellites (EUMETSAT)/Europe.
- European Telecommunications Satellite Organization (EUTELSAT)/Europe.
- Geo-Informatics and Space Technology Development Agency (GISTDA)/Thailand.
- Hellenic National Space Committee (HNSC)/Greece.
- Hellenic Space Agency (HSA)/Greece.
- Indian Space Research Organization (ISRO)/India.
- Institute of Space Research (IKI)/Russian Federation.
- Korea Aerospace Research Institute (KARI)/Korea.
- Ministry of Communications (MOC)/Israel.
- Mohammed Bin Rashid Space Centre (MBRSC)/United Arab Emirates.
- National Institute of Information and Communications Technology (NICT)/Japan.
- National Oceanic and Atmospheric Administration (NOAA)/USA.
- National Space Agency of the Republic of Kazakhstan (NSARK)/Kazakhstan.
- National Space Organization (NSPO)/Chinese Taipei.
- Naval Center for Space Technology (NCST)/USA.
- Research Institute for Particle & Nuclear Physics (KFKI)/Hungary.
- Scientific and Technological Research Council of Turkey (TUBITAK)/Turkey.
- South African National Space Agency (SANSA)/Republic of South Africa.
- Space and Upper Atmosphere Research Commission (SUPARCO)/Pakistan.
- Swedish Space Corporation (SSC)/Sweden.
- Swiss Space Office (SSO)/Switzerland.
- United States Geological Survey (USGS)/USA.

CCSDS REPORT CONCERNING DELTA-DOR—
TECHNICAL CHARACTERISTICS AND PERFORMANCE

DOCUMENT CONTROL

Document	Title	Date	Status
CCSDS 500.1-G-1	Delta-DOR—Technical Characteristics and Performance, Informational Report, Issue 1	May 2013	Original issue, superseded
CCSDS 500.1-G-2	Delta-DOR—Technical Characteristics and Performance, Informational Report, Issue 2	November 2019	Current issue

CONTENTS

<u>Section</u>	<u>Page</u>
1 INTRODUCTION	1-1
1.1 PURPOSE AND SCOPE.....	1-1
1.2 APPLICABILITY.....	1-1
1.3 COMMON DELTA-DOR TERMINOLOGY.....	1-1
1.4 STRUCTURE OF THIS DOCUMENT.....	1-2
1.5 REFERENCES.....	1-2
2 OVERVIEW OF THE DELTA-DOR TECHNIQUE	2-1
2.1 SPACECRAFT AND QUASAR OBSERVATIONS.....	2-1
2.2 THE MEASUREMENT OF SPACECRAFT AND QUASAR SIGNALS.....	2-2
2.3 OBSERVATION SEQUENCES.....	2-3
2.4 OBSERVABLE MODELING.....	2-3
2.5 DELTA-DOR REQUIREMENTS ON SPACE AND GROUND INFRASTRUCTURE.....	2-3
2.6 DELTA-DOR INTERFACES.....	2-5
3 SPACECRAFT SIGNAL STRUCTURE	3-1
3.1 OVERVIEW.....	3-1
3.2 SINUSOIDAL SIDEBANDS.....	3-1
3.3 SPREAD SPECTRUM SIDEBANDS.....	3-4
3.4 AMBIGUITY RESOLUTION.....	3-8
4 THEORETICAL BACKGROUND	4-1
4.1 MEASUREMENT EQUATIONS.....	4-1
4.2 DELTA-DOR AS A NAVIGATION TECHNIQUE.....	4-7
4.3 THE DELTA-DOR ERROR BUDGET.....	4-8
5 SYSTEM RATIONALE AND TRADE-OFFS	5-1
5.1 DEFINITION OF PARAMETERS USED IN DELTA-DOR TRADE-OFFS.....	5-1
5.2 TRADE-OFF ON SPACECRAFT TONE POWER.....	5-6
5.3 THE ACHIEVABLE PERFORMANCE – X-BAND.....	5-8
5.4 THE ACHIEVABLE PERFORMANCE – KA-BAND.....	5-10

CONTENTS (continued)

<u>Section</u>	<u>Page</u>
6 DESCRIPTION OF EXISTING SYSTEMS	6-1
6.1 THE NASA SYSTEM	6-1
6.2 THE ESA SYSTEM	6-4
6.3 THE JAXA SYSTEM	6-7
ANNEX A SPREAD SPECTRUM DOR CODE PARAMETERS	A-1
ANNEX B ABBREVIATIONS AND ACRONYMS	B-1

Figure

2-1 Delta-DOR Observation Geometry	2-1
2-2 Block Diagram of Major Components of Delta-DOR Ground System	2-4
2-3 High-Level Delta-DOR Flow	2-6
3-1 Illustration of Instrumental Error Due to Phase Dispersion within a Recording Channel	3-5
3-2 Spectra of Quasar and Spacecraft DOR Signals	3-6
4-1 VLBI Geometry for Two Receivers and One Radio Source	4-1
4-2 Differential VLBI Geometry for Two Receivers and Two Radio Sources	4-2
4-3 Downlink Tone Spectrum and Coincident VLBI Channels	4-3
4-4 Delta-DOR Error Budget for X-Band Including Random and Systematic Effects (1 Sigma)	4-19
5-1 Estimated Delta-DOR Performance, 1 Sigma, at X-Band As a Function of Spacecraft-Quasar Separation Angle	5-10
5-2 Estimated Delta-DOR Performance, 1 Sigma, at Ka-Band As a Function of Spacecraft-Quasar Separation Angle	5-14
6-1 Simplified Block Diagram of Delta-DOR System in the NASA Deep Space Network	6-3
6-2 Simplified Block Diagram of Delta-DOR System in the ESA Deep Space Network (New Norcia S-Band Not Shown)	6-6
6-3 Simplified Block Diagram of Delta-DOR Back-End System in the JAXA Stations ...	6-9
A-1 SRRC Filter Response for a Variety of Roll-Off Factors	A-3
A-2 Trade Between Chip Rate and Roll-Off Facto	A-4
A-3 PN Spectrum Shaping As a Result of an Analog LPF, 200 MHz Bandwidth	A-4
A-4 PN Spectrum As a Result of an Analog LPF, 36 MHz Bandwidth	A-5
A-5 PN Spectrum Flattened by Equalization/Pre-Distortion Filter, 36 MHz Bandwidth	A-5
A-6 Recommended X-Band Gold Code Generator Circuit	A-7
A-7 Recommended Ka-Band Gold Code Generator Circuit	A-7

CONTENTS (continued)

<u>Table</u>	<u>Page</u>
4-1 Nominal Parameter Values [Typical NASA Case] for Evaluation of Δ DOR Error Budget.....	4-17
4-2 Delta-DOR Error Budget (1 Sigma)—Both Random and Systematic Effects	4-20
4-3 Delta-DOR Error Budget (1 Sigma)—Random Effects Only	4-20
4-4 Delta-DOR Error Budget (1 Sigma)—Systematic Effects Only	4-21
5-1 Dependence of Delay Precision and Accuracy on Spacecraft Signal Parameters: High Performance Case	5-7
5-2 Dependence of Delay Precision and Accuracy on Spacecraft Signal Parameters: Low Gain Antenna Case.....	5-7
5-3 Dependence of Delay Precision and Accuracy on Spacecraft Signal Parameters: No DOR Tone or Low Frequency DOR Tone Case.....	5-8
5-4 Nominal Parameter Values for Evaluation of Δ DOR Trade-Offs at X-Band	5-8
5-5 Nominal Parameter Values for Evaluation of Δ DOR Trade-Offs at Ka-Band.....	5-13
6-1 Functional Specifications for the NASA Delta-DOR System.....	6-2
6-2 Functional Specifications for the ESA Delta-DOR System	6-5
6-3 Functional Specifications for the JAXA Delta-DOR System (Usuda Station)	6-8
A-1 Recommended Chip Rate and Roll-Off Factors	A-6
A-2 Recommended Code Length.....	A-6
A-3 Recommended Gold Code Polynomials	A-6

1 INTRODUCTION

1.1 PURPOSE AND SCOPE

This Informational Report describes the theoretical aspects of and discusses trade-offs and system performance for the navigation technique known as Delta Differential One-Way Ranging (Delta-DOR or Δ DOR). It has been developed via consensus of the Delta-DOR Working Group of the CCSDS Systems Engineering Area (SEA). Tracking data including Delta-DOR may be exchanged between CCSDS Member Agencies during cross support of space missions.

Delta-DOR is a technique, derived from Very Long Baseline Interferometry (VLBI), that can be used in conjunction with Doppler and ranging data to improve spacecraft navigation by more efficiently determining spacecraft angular position in the plane of sky. The establishment of interoperability for acquiring and processing Delta-DOR data at ground stations of different agencies, the standardization of service requests for Delta-DOR, the standardization of an exchange format for raw data, and standardization of interfaces for exchange of supporting products are key enablers for interagency execution of Delta-DOR operations. The interfaces relevant for interagency Delta-DOR and the supporting CCSDS standards are discussed in 2.6.

Conventions and definitions of Delta-DOR concepts are provided in this report. A detailed description of the Delta-DOR technique is provided, including guidelines for DOR tone spectra, guidelines for selecting reference sources, applicable foundation equations, and a discussion of error sources and measurement accuracy.

1.2 APPLICABILITY

Delta-DOR operations are applicable to space agencies that operate deep space missions that require accurate determination of the spacecraft position in the plane of the sky. Accurate position determinations are often needed in critical mission phases such as planetary encounters and flybys. For operations in which these requirements do not capture the needs of the participating agencies, Delta-DOR operations may not be appropriate.

1.3 COMMON DELTA-DOR TERMINOLOGY

Part of the standardization process involves the determination of common interagency terminology. The following terminology is used in this informational report and in related Delta-DOR standards.

Term	Meaning
baseline	The vector joining two tracking stations
channel	A slice of the frequency spectrum that contains a spacecraft or quasar signal

CCSDS REPORT CONCERNING DELTA-DOR—
TECHNICAL CHARACTERISTICS AND PERFORMANCE

Term	Meaning
scan	An observation of a radio source, typical duration of a few minutes
session	The time period of the Delta-DOR measurement including several scans
spanned bandwidth	The widest frequency separation between downlink signal components
DOR Tone	Tone generated by a spacecraft for purpose of enabling Delta-DOR measurement; more generally, any spacecraft signal component used for Delta-DOR
P_T/N_0	Total power to noise spectral density ratio
P_{Tone}/N_0	Tone power to noise spectral density ratio
G/T	Ratio of antenna gain to system noise temperature
meteo data	Meteorological data (consists of pressure, temperature, relative humidity)

1.4 STRUCTURE OF THIS DOCUMENT

In addition to this section, this document contains the following sections and annex:

- Section 2 provides a general overview of the Delta-DOR technique.
- Section 3 provides the spacecraft signal structure.
- Section 4 provides a theoretical background for the technique.
- Section 5 describes system rationale and trade-offs.
- Section 6 provides descriptions of existing systems.
- Annex A is a list of abbreviations and acronyms applicable to Delta-DOR.

1.5 REFERENCES

The following documents are referenced in this Report. At the time of publication, the editions indicated were valid. All documents are subject to revision, and users of this Report are encouraged to investigate the possibility of applying the most recent editions of the documents indicated below. The CCSDS Secretariat maintains a register of currently valid CCSDS documents.

- [1] A. Richard Thompson, James M. Moran, and George W. Swenson, Jr. *Interferometry and Synthesis in Radio Astronomy*. 3rd ed. Cham, Switzerland.: Springer, 2017.

CCSDS REPORT CONCERNING DELTA-DOR—
TECHNICAL CHARACTERISTICS AND PERFORMANCE

- [2] A. E. E. Rogers. “Very-Long-Baseline Interferometry with Large Effective Bandwidth for Phase-Delay Measurements.” *Radio Science* 5, no. 10 (Oct. 1970): 1239–1247.
- [3] Theodore D. Moyer. *Formulation for Observed and Computed Values of Deep Space Network Data Types for Navigation*. JPL Deep-Space Communications and Navigation Series. Joseph H. Yuen, Series Editor. Hoboken, N.J.: Wiley, 2003.
- [4] *IERS Conventions (2003)*. Edited by Dennis D. McCarthy and Gérard Petit. IERS Technical Note No. 32. Frankfurt am Main, Germany: Bundesamt für Kartographie und Geodäsie, 2004.
- [5] *Radio Frequency and Modulation Systems—Part 1: Earth Stations and Spacecraft*. Issue 29. Recommendations for Space Data System Standards (Blue Book), CCSDS 401.0-B-29. Washington, D.C.: CCSDS, March 2019.
- [6] *X-Band Radio Source Catalog*. Module 107D in *DSN Telecommunications Link Design Handbook*. DSN No. 810-005. Pasadena California: JPL, October 22, 2015.
- [7] *Navigation Data—Definitions and Conventions*. Report Concerning Space Data System Standards, CCSDS 500.0-G-3. Green Book. Issue 3. Washington, D.C.: CCSDS, May 2010.
- [8] John A. Klobuchar. *A First-Order, Worldwide, Ionospheric, Time-Delay Algorithm*. Air Force Surveys in Geophysics, AFCRL-TR-75-0502. Hanscom AFB, Massachusetts: Ionospheric Physics Laboratory, Air Force Cambridge Research Laboratories, 1975.
- NOTE – The relevant material in this reference can also be found in section 10.3 of reference [3].
- [9] P. S. Callahan. “An Analysis of Viking S-X Doppler Measurements of Solar Wind Columnar Content Fluctuations.” *DSN Progress Report* 42-44, January-February 1978 (April 15, 1978): 75–81.
- [10] C. Ma, et al. “The Second Realization of the International Celestial Reference Frame by Very Long Baseline Interferometry.” *IERS Technical Note*. No. 35. Frankfurt am Main: Verlag des Bundesamts für Kartographie und Geodäsie, 2009.
- NOTE – Reference for ICRF3 to be published soon.
- [11] *Delta-Differential One Way Ranging (Delta-DOR) Operations*. Issue 2. Recommendation for Space Data System Practices (Magenta Book), CCSDS 506.0-M-2. Washington, D.C.: CCSDS, February 2018.
- [12] *Delta Differential One-way Ranging*. Module 210, Rev. C, June 6, 2019 in *DSN Telecommunications Link Design Handbook*. DSN No. 810-005, Rev. E. Pasadena California: JPL, November 30, 2000.

CCSDS REPORT CONCERNING DELTA-DOR—
TECHNICAL CHARACTERISTICS AND PERFORMANCE

- [13] *Delta-DOR Raw Data Exchange Format*, Recommendation for Space Data System Standards, CCSDS 506.1-B-1. Blue Book. Issue 1. Washington, D.C.: CCSDS, June 2013.
- [14] W. Majid and D. Bagri. “Availability of Calibration Sources for Measuring Spacecraft Angular Position with Sub-Nanoradian Accuracy.” *IPN Progress Report* 42-165 (May 15, 2006).
- [15] J. M. Wrobel, et al. “Faint Radio Sources in the NOAO Boötes Field: VLBA Imaging and Optical Identifications.” *AJ* 130, no. 3 (Sep. 2005): 923–935.
- [16] A. J. Beasley, et al. “The VLBA Calibrator Survey—VCS1.” *ApJS* 141, no. 1 (July 2002): 13–21.
- [17] D. Morabito, R. Clauss, and M. Speranza. “Ka-Band Atmospheric Noise-Temperature Measurements at Goldstone, California, Using a 34-Meter Beam-Waveguide Antenna.” *TDA Progress Report* 42-132, October-December 1997 (February 15, 1998): 1–20.
- [18] *34-m BWG Stations Telecommunications Interfaces*. Module 104J in *DSN Telecommunications Link Design Handbook*. DSN No. 810-005. Pasadena California: JPL, January 12, 2018.
- [19] *Atmospheric and Environmental Effects*. Module 105E in *DSN Telecommunications Link Design Handbook*. DSN No. 810-005. Pasadena California: JPL, October 22, 2015.
- [20] G. E. Lanyi, et al. “The Celestial Reference Frame at 24 and 43 GHz. I. Astrometry.” *AJ* 139, no. 5 (May 2010): 1695–1712.
- [21] P. Charlot, et al. “The Celestial Reference Frame at 24 and 43 GHz. II. Imaging.” *AJ* 139, no. 5 (May 2010): 1713–1770.
- [22] “VLBI Standard Interface (VSI).” VLBI Standards & Resources Website. <http://vlbi.org/vsi/>.
- [23] “Assignment of Differential One-Way Ranging Tone Frequencies for Category B Missions.” In *Handbook of the Space Frequency Coordination Group*, Recommendation SFCG 23-2, 25 September, 2003. Noordwijk, The Netherlands: SFCG, 2012.
- [24] “Use of Differential One Way Ranging Tones in the 8400-8450 MHz Band for Category-B SRS Missions.” In *Handbook of the Space Frequency Coordination Group*, Recommendation SFCG 30-1, 14 July, 2010. Noordwijk, The Netherlands: SFCG, 2012.
- [25] *Extensible Space Communication Cross Support—Service Management—Concept*. Report Concerning Space Data System Standards, CCSDS 902.0-G-1. Green Book. Issue 1. Washington, D.C.: CCSDS, September 2014.

CCSDS REPORT CONCERNING DELTA-DOR—
TECHNICAL CHARACTERISTICS AND PERFORMANCE

- [26] *Tracking Data Message*. Recommendation for Space Data System Standards, CCSDS 503.0-B-1. Blue Book. Issue 1. Washington, D.C.: CCSDS, November 2007.
- [27] *Orbit Data Messages*. Recommendation for Space Data System Standards, CCSDS 502.0-B-2. Blue Book. Issue 2. Washington, D.C.: CCSDS, November 2009.
- [28] D. Curkendall and J. Border. "Delta-DOR: The One-Nanoradian Navigation Measurement System of the Deep Space Network—History, Architecture, and Componentry." *Interplanetary Network Progress Report*, 42-193 (2013): 1-46.
- [29] R. Treuhaft and S. Lowe, "A Nanoradian Differential VLBI Tracking Demonstration." *Telecommunications and Data Acquisition Progress Report*, 42-109 (1992): 40-55, May 15.
- [30] S. Lowe, "A Measurement of X-Band Front-End Phase Dispersion for Delta-Differenced One-Way Range (DDOR) Experiments." *Interplanetary Network Progress Report*, 42-184 (2011): 1-15.
- [31] M. Mercolino, et al. "A 1 nrad Delta-DOR System." Presented at *TTC 2016: 7th ESA International Workshop on Tracking, Telemetry and Command Systems for Space Applications* (13-16 September 2016, Noordwijk, The Netherlands).
- [32] *Data Transmission and PN Ranging for 2 GHz CDMA Link via Data Relay Satellite*. Issue 1. Recommendation for Space Data System Standards (Blue Book), CCSDS 415.1-B-1. Washington, D.C.: CCSDS, September 2011.
- [33] *Delta-DOR Raw Data Exchange Format*. Issue 1. Recommendation for Space Data System Standards (Blue Book), CCSDS 506.1-B-1. Washington, D.C.: CCSDS, June 2013.
- [34] *Delta-Differential One Way Ranging (Delta-DOR) Operations*. Issue 2. Recommendation for Space Data System Practices (Magenta Book), CCSDS 506.0-M-2. Washington, D.C.: CCSDS, February 2018.

2 OVERVIEW OF THE DELTA-DOR TECHNIQUE

2.1 SPACECRAFT AND QUASAR OBSERVATIONS

VLBI is a technique that allows determination of angular position for distant radio sources by measuring the geometric time delay between received radio signals at two geographically separated stations. The observed time delay is a function of the known baseline vector joining the two radio antennas and the direction to the radio source.

An application of VLBI is spacecraft navigation in space missions in which delay measurements of a spacecraft radio signal are compared against similar delay measurements of angularly nearby quasar radio signals. In the case in which the spacecraft measurements are obtained from the phases of tones emitted from the spacecraft, first detected separately at each station and then differenced, this application of VLBI is known as Delta Differential One-Way Ranging. The observation geometry is illustrated in figure 2-1. Even though data acquisition and processing are not identical for the spacecraft and quasar, both types of measurements can be interpreted as delay measurements, and they have similar information content and similar sensitivity to sources of error. The data produced in such a measurement session are complementary to Doppler and ranging data.

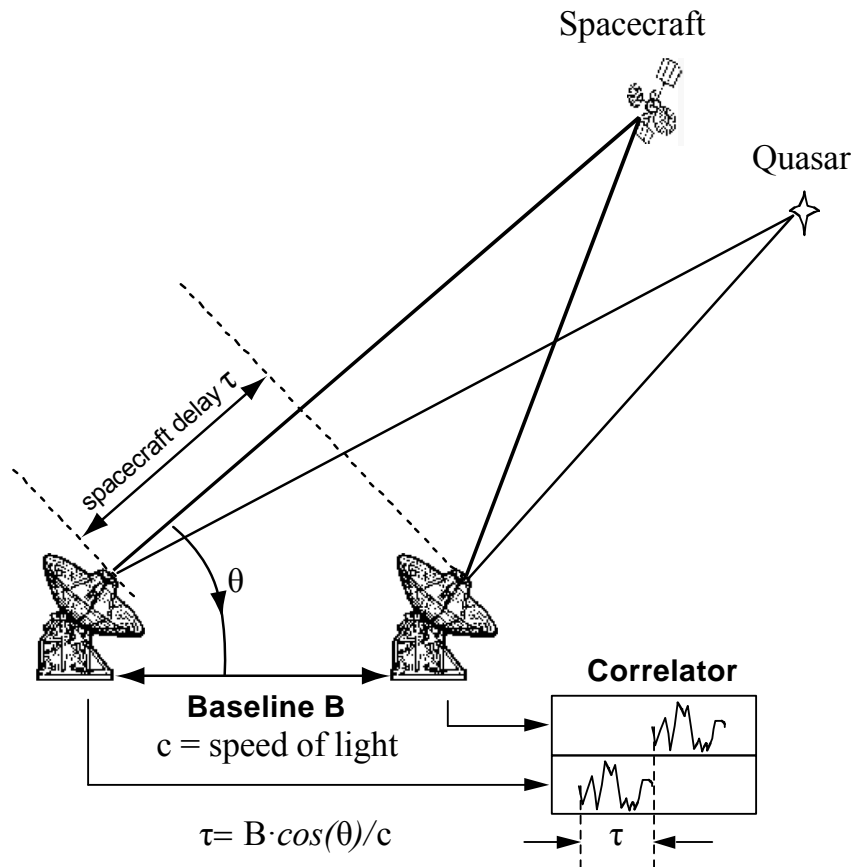


Figure 2-1: Delta-DOR Observation Geometry

To enable a Delta-DOR measurement, a spacecraft must emit several tones or other signal components spanning at least a few MHz. The characteristics of the tones are selected based on the requirements for phase ambiguity resolution, measurement accuracy, efficient use of spacecraft signal power, efficient use of ground tracking resources, and the frequency allocation for space research.

The Delta-DOR technique requires that spacecraft be tracked simultaneously at two distinct radio antennas. A quasar must also be tracked simultaneously just before and/or after the spacecraft observation. Thus a viewing overlap between the two antenna complexes is required; the degree of overlap varies for each pair of antenna complexes and depends on the relative station locations and on spacecraft declination.

The Delta-DOR history, technique, and applications are discussed in reference [28].

2.2 THE MEASUREMENT OF SPACECRAFT AND QUASAR SIGNALS

Data acquisition must first be coordinated between stations; it then occurs independently at each station. Data are recorded using an open loop receiver at each station and sent to a common correlator facility for processing. It is generally not practical to transfer and correlate data in real time when stations are widely separated, as is the case for Delta-DOR. Data must be recorded in selected frequency channels that include signals received from the spacecraft. Generally, three or more channels spanning at least a few MHz are recorded. Data from the quasar(s) must also be recorded in similar channels. The recording is of the voltage of the received electromagnetic signal from the antenna feed, after downconversion and filtering.

The spacecraft delay is obtained in this application by first making a one-way range measurement at each station. The one-way range is determined for a single station by extracting the phases of two or more emitted signals. The signals emitted for this purpose are referred to as DOR tones. A DOR observable is generated by subtracting the one-way range measurements from two stations at a common reception time. While each one-way range measurement is affected by the unknown offset in the spacecraft clock, the station-differencing eliminates this effect. However, DOR measurements are still biased by ground station clock offsets and instrumental delays. DOR measurements are quite similar technically to interferometric delay measurements and, when convenient, are referred to in this document as spacecraft delay measurements.

For measuring the quasar, each station is configured to acquire data from it in frequency channels centered on the spacecraft tone frequencies. This receiver configuration choice ensures that the spacecraft-quasar differencing eliminates the effects of ground station clock offsets and instrumental delays. By selecting a quasar that is close in an angular sense to the spacecraft, and by observing the quasar at nearly the same time as the spacecraft, the effects of errors in the modeled station locations, Earth orientation, and transmission media delays are also diminished.

2.3 OBSERVATION SEQUENCES

Normally, a Delta-DOR pass consists of three or more scans of data recording, each of a few minutes duration. A scan consists of pointing the antennas to one radio source and recording the signal. The antennas must slew to another radio source for the next scan, and so on. The observing sequence is spacecraft-quasar-spacecraft, quasar-spacecraft-quasar, or a longer sequence of alternating observations, depending on the characteristics of the radio sources and the objectives of the measurement session. A minimum of three scans is required to eliminate clock-epoch and clock-rate offsets and then measure spacecraft angular position. Normally a three-scan sequence is repeated several times. Once collected, the received signals are brought to a common site and correlated. The observed quantity in a Delta-DOR observation is time delay for each radio source.

2.4 OBSERVABLE MODELING

In navigation processing, the delay or DOR observable is modeled for each scan of each radio source. The measured observable depends on both geometric factors and on delays introduced by transmission media. Meteo data are provided from each tracking site so that, possibly in conjunction with other data such as Global Positioning System (GPS) measurements, corrections can be computed to account for tropospheric and ionospheric path delays. The modeled or ‘computed’ observable is based on a nominal spacecraft trajectory, geometric parameters, and available calibrations for tropospheric and ionospheric delays. Residuals are formed by subtracting the computed observables from the measured time delay values. The ‘Delta’ between spacecraft and quasar observations is generated internal to the navigation processing by subtracting residual values of quasar observations from residual values of spacecraft observations. These data are used in conjunction with other data to solve for a correction to the spacecraft trajectory.

2.5 DELTA-DOR REQUIREMENTS ON SPACE AND GROUND INFRASTRUCTURE

Because each Delta-DOR measurement requires the use of two antennas, and navigation accuracy is improved by baseline diversity, this technique is highly conducive to interagency cooperation. Measurements from two baselines are required to determine both components of angular position, with orthogonal baselines providing the best two-dimensional coverage. While most agencies do not have enough station complexes to provide orthogonal baselines by themselves, the existing assets of more than one agency today could provide two or more pairs of angularly separated baselines and good geometric coverage for missions throughout the ecliptic plane. Stations from different agencies can be used as Delta-DOR data collectors for navigation purposes, assuming that the infrastructure has been laid to facilitate such cooperation.

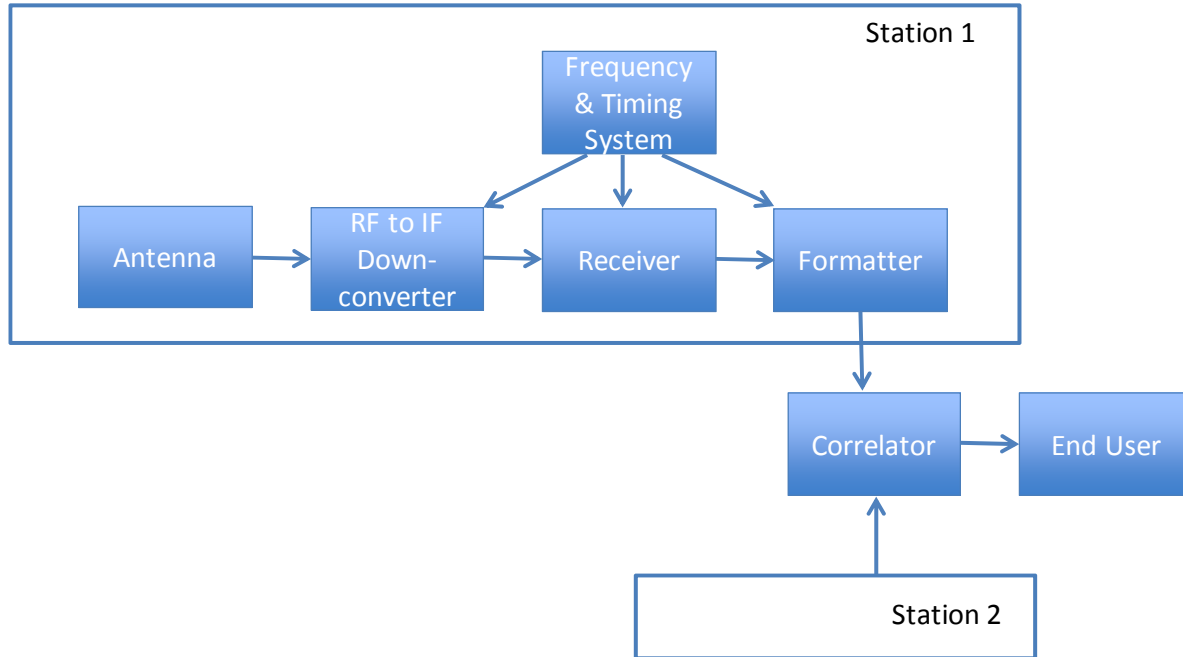


Figure 2-2: Block Diagram of Major Components of Delta-DOR Ground System

The major components of a Delta-DOR ground system are shown in figure 2-2. Signals are received by an antenna, processed through ground-station electronics, and recorded in a digital format. Data from two or more stations are sent to a common correlator facility where time delay observables are derived. The observables are passed on to an end user. The required interfaces are discussed in 2.6.

While natural radio sources generate broadband signals to enable such a measurement, the spacecraft transponder must also include the specific capability to emit signals spanning a wide bandwidth. Requirements on spacecraft signal structure are given in the Radio Frequency and Modulation Systems Standard (reference [5]).

Received signals are typically weak because of the limited power available for spacecraft transmissions and the vast distances to the quasars. Therefore large antennas with good sensitivity are necessary for data acquisition. Precise clocks and stable frequency distribution must be used within a station to avoid degradation of time delay measurements. The station coordinates must be well known, and media delays for received signals must be well calibrated. Because of the signal weakness, and in order not to introduce unwanted delays or phase instabilities, it is necessary that the signal path from front end to control room be well known and stable.

Good knowledge of timing and high frequency stability is, and has been, enabling capabilities for radio interferometric systems with components separated by large distances. Generally, the level of stability provided by a Hydrogen Maser is necessary to support these measurements.

An open loop recording system must be used, at least for signals from natural radio sources, since the received noise cannot be modeled or compressed. A large data volume must be recorded to build sensitivity for weak quasar signals. This large data volume must then be transferred, from each station, to the common correlator site. A typical data volume per session may be 10 to 40 GBytes at each station, though this could vary quite a bit depending on circumstance. The ability to transfer data volumes of this size rapidly may be needed in support of time critical navigation events. A high-speed network connection is generally used to meet latency requirements. The correlator output is provided to the end user, which is usually a flight dynamics team.

Data are recorded in multiple frequency channels, centered on the received frequencies of spacecraft tones. There are three different parameters related to bandwidth involved, and performance generally improves as each of these parameters is increased:

- a) the single frequency channel, which has a bandwidth typically in the range of 2 to 8 MHz for quasar signals;
- b) the data rate for a recorder, which is the product of the channel bandwidth times 2 (for Nyquist sampling) times the number of bits per sample times the number of channels (a given recorder will have a maximum sample rate, so selection of channels will be constrained);
- c) the spanned bandwidth, which is the frequency separation between the two widest-spaced channels.

A correlator facility is needed for processing of data. This basically consists of a computer server, a high-speed network connection, and application software for data correlation.

Conceptually, for the best performance, a spacecraft would transmit a signal that filled the largest possible band, and each station would record the full band, but this is not practical, or even allowable, for several different reasons. Much of the rest of this report provides trade-offs and analysis toward achieving high performance given constraints on bandwidth.

2.6 DELTA-DOR INTERFACES

The high-level Delta-DOR data flow below shows various interfaces (numbered 1 through 7 in figure 2-3) in which standardization is beneficial in terms of establishing interoperability. Figure 2-3 also shows the functions that must be performed by one or more Agency.

In general, an interface exists or is defined to cover the necessary parameters at each stage of the data flow. During data acquisition, radio source signals that arrive at an antenna are detected by a receiver (Rx), and then stored at the site. Next, data from at least two sites are transferred to a central location and correlated to generate observables. Finally, uncalibrated reduced data (i.e., time delay observables) and meteo data to be used to calibrate path delays through transmission media provided to the Orbit Determination.

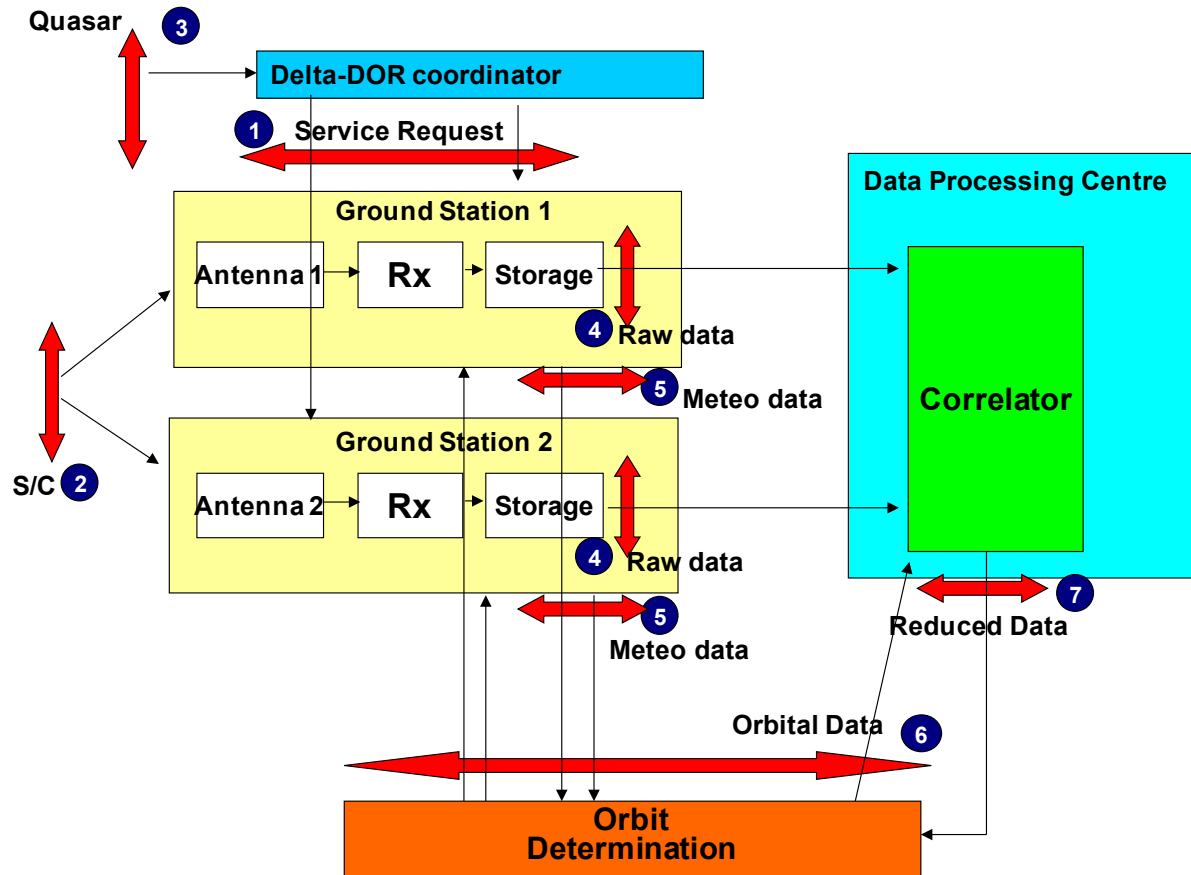


Figure 2-3: High-Level Delta-DOR Flow

With reference to figure 2-3 the following interfaces can be defined:

- IF-1: Service Request, including observation schedule and sequence. This interface is defined in reference [34] and is managed according to reference [25].
- IF-2: DOR signal for S/C tracking. This interface is defined in reference [5].
- IF-3: quasar catalogue for Delta-DOR (reference [6]). The catalogue provides quasar coordinates and flux that are used for measurement planning.
- IF-4: exchange format for raw Delta-DOR data. This interface is standardized in reference [13] and may differ from the native format used for raw data by an Agency.
- IF-5: meteo data. Meteo data may include information on temperature, pressure, relative humidity, tropospheric delay, and ionospheric delay. This interface is defined by the Tracking Data Message (TDM) (reference [26]).
- IF-6: orbital data. These data are used at all stations to define antenna pointing during data acquisition and received frequency predictions. These data are also input to the Delta-DOR correlator. This input relies on the S/C orbit prediction, and therefore

CCSDS REPORT CONCERNING DELTA-DOR—
TECHNICAL CHARACTERISTICS AND PERFORMANCE

information is exchanged among agencies via Orbit Ephemeris Message (OEM) products (reference [27]).

- IF-7: reduced data. These are the products of the Delta-DOR, which normally consist of S/C DOR, quasar DOR, and clock bias. This interface is defined by the TDM (reference [26]).

3 SPACECRAFT SIGNAL STRUCTURE

3.1 OVERVIEW

A spacecraft transponder must emit a signal spanning a bandwidth of at least a few megahertz to enable a DOR measurement. Up to the present time, sinusoidal sidebands, referred to as DOR tones, have primarily been used for DOR measurements. Spread spectrum sidebands have also been considered. This section provides information and options on the signal structure needed to enable a DOR measurement.

3.2 SINUSOIDAL SIDEBANDS

3.2.1 GENERAL

Recommended Standards for sinusoidal DOR tones are given in reference [5]. The DOR tones are generated by modulating a sine wave or square wave onto the downlink carrier. Requirements on the number of DOR tones, tone frequencies, and tone power are based on the expected *a priori* knowledge of spacecraft angular position and on the required differential range measurement accuracy, as discussed in section 3 of this document. Generally, a narrow-spanned bandwidth is needed to resolve the integer cycle phase ambiguity in the observed signals based on *a priori* knowledge of spacecraft angular position, while a wide-spanned bandwidth is needed for high measurement accuracy.

The use of harmonic tones generated by modulating the carrier signal by a single tone provides a low performance option. As tone power drops off for the higher harmonics, the maximum-spanned bandwidth is usually just a few times the fundamental frequency, so a wide-spanned bandwidth may not be possible when using single-tone modulation. To provide higher performance (i.e., a wider spanned bandwidth with more power in the outer tones) while still providing a spanned bandwidth narrow enough for integer-cycle phase-ambiguity resolution, more DOR tones are needed. Sine waves are normally used in multi-tone systems based on efficiency considerations. Once the ambiguity has been resolved for one channel pair, it is generally possible then to resolve the ambiguity for a channel pair with twenty to eighty times the spanned bandwidth of the first pair.

For example, Δ DOR measurements were made for the Voyager spacecraft using high order harmonics of the 360 kHz telemetry square wave subcarrier signal. More accurate Δ DOR measurements were made of the Mars Observer spacecraft using two sine wave signals (3.825 MHz and 19.125 MHz) modulated onto the downlink carrier.

It is preferable for DOR tones to be frequency coherent with the downlink carrier. This facilitates the detection of weak DOR tones by allowing the use of a phase model derived from the received carrier signal. Also, the transmitted spanned bandwidth of the DOR tones, which must be known for the generation of a differential range observable from received phase measurements, will in this case be a defined multiple of the transmitted carrier frequency.

The most usual sinusoidal DOR tone modulation formats are presented next.

3.2.2 DOR TONES GENERATED FROM MODULATION BY TWO SINE WAVES

Two sinusoidal tones with angular frequencies ω_1 and ω_2 are phase modulated on the downlink carrier signal with peak modulation indices m_1 and m_2 , respectively:

$$s(t) = \sqrt{2P_T} \cos(\omega_c t + m_1 \sin(\omega_1 t) + m_2 \sin(\omega_2 t)). \quad (1)$$

The above expression may be expanded to separate the carrier and main DOR tone components of the signal from higher-order harmonics:

$$s(t) = \sqrt{2P_T} [J_0(m_1)J_0(m_2)\cos(\omega_c t) - 2J_1(m_1)J_0(m_2)\sin(\omega_c t)\sin(\omega_1 t) - \\ 2J_0(m_1)J_1(m_2)\sin(\omega_c t)\sin(\omega_2 t) + \text{higher harmonics}] \quad (2)$$

where J_0 and J_1 are Bessel functions of the first kind. The modulation produces tones at frequencies of $\omega_c \pm \omega_1$ and $\omega_c \pm \omega_2$. Modulation indices may be chosen to put more power in the outer tones while putting just enough power in the inner tones to provide for ambiguity resolution.

The powers allocated to the carrier and the tones are easily deduced from the above expression:

$$P_c = P_T J_0^2(m_1) J_0^2(m_2), \\ P_1 = P_T J_1^2(m_1) J_0^2(m_2), \text{ and} \\ P_2 = P_T J_0^2(m_1) J_1^2(m_2). \quad (3)$$

The corresponding modulation losses are expressed as the fractions below:

$$\frac{P_c}{P_T} = J_0^2(m_1) J_0^2(m_2), \\ \frac{P_1}{P_T} = J_1^2(m_1) J_0^2(m_2), \text{ and} \\ \frac{P_2}{P_T} = J_0^2(m_1) J_1^2(m_2). \quad (4)$$

The above two-sine-wave signaling scheme was used on Mars Observer. For Mars Observer, the nominal values of the DOR modulation indices are $m_1=0.64$ rad and $m_2=0.32$ rad for the $f_1=19.125$ MHz and $f_2=3.825$ MHz DOR tones, respectively. Such values yield modulation losses $P_c/P_T=-1.14$ dB, $P_1/P_T=-10.57$ dB, and $P_2/P_T=-16.94$ dB.

Annex A describes a design methodology for the various parameters that define a PN Code and presents a recommended set of parameters to optimize Δ DOR performance.

3.2.3 DOR TONES GENERATED FROM MODULATION BY ONE SQUARE WAVE

In this case, one square-wave signal with unit amplitude and frequency ω_1 is phase modulated on the downlink carrier to generate a downlink signal with multiple tones:

$$s(t) = \sqrt{2P_T} \cos(\omega_c t + m_1 \text{sqwv}(\omega_1 t)). \quad (5)$$

The cosine of the sum may be expanded to give:

$$s(t) = \sqrt{2P_T} \cos(m_1 \text{sqwv}(\omega_1 t)) \cos(\omega_c t) - \sqrt{2P_T} \sin(m_1 \text{sqwv}(\omega_1 t)) \sin(\omega_c t). \quad (6)$$

The second term on the right-hand side is a carrier signal multiplied by a square wave with amplitude $\sin(m_1)$. This square wave has a Fourier expansion,

$$\sin(m_1 \text{sqwv}(\omega_1 t)) = \sin(m_1) \frac{4}{\pi} \sum_{k=1}^{\infty} \frac{\cos[(2k-1)\omega_1 t]}{2k-1}, \quad (7)$$

and equation (6) may be rewritten as

$$s(t) = \sqrt{2P_T} \cos(m_1 \text{sqwv}(\omega_1 t)) \cos(\omega_c t) - \sqrt{2P_T} \sin(m_1) \frac{4}{\pi} \sum_{k=1}^{\infty} \frac{\cos[(2k-1)\omega_1 t]}{2k-1} \sin(\omega_c t). \quad (8)$$

The second term on the right-hand side produces tones at odd multiples of the subcarrier frequency spaced about the carrier. The modulation loss formula for the square-wave harmonics is easily calculated from the coefficients of the above expression:

$$\frac{P_k}{P_T} = \frac{4}{\pi^2} \frac{1}{(2k-1)^2} \sin^2(m_1) \text{ at } \omega_c \pm (2k-1)\omega_1 \text{ for } k = 1, 2, 3, \dots \quad (9)$$

Considering that the cosine is an even function, the first term on the right-hand side of equation (7) would appear to produce a pure carrier signal with $P_c/P_T = \cos^2(m_1)$. However, since the square wave must be band limited, the function $\cos(m_1 \text{sqwv}(\omega_1 t))$ is actually a spike train with period $2\pi/(2\omega_1)$ and amplitude $(1 - \cos m_1)$. This spike train produces even harmonics of the square wave frequency about the carrier signal. For high-rate subcarriers, these tones may be detectable and usable as DOR tones. The power in the even harmonics is proportional to $(1 - \cos m_1)^2$, but the actual power depends on the shape of the subcarrier signal. The total power in the even harmonics, excluding the carrier signal itself, is usually quite small.

When telemetry modulation is imposed on the subcarrier, the odd harmonics are spread. The even harmonics generated from the spike train, on the other hand, remain as pure tones. High-order even harmonics of the high-rate telemetry subcarrier, at a level of about -30 dB relative to the total signal power, were used as DOR tones for the Voyager and Magellan

spacecraft. While such measurements of opportunity may be useful, it is difficult to plan for this case since the spectrum depends on the precise shape of the subcarrier signal.

Normally, low-order odd harmonics of the square wave modulation would serve as DOR tones. This scheme was used on the Vega and Phobos missions.

As an example, for a fully suppressed carrier ($m_f=90$ degrees), the suppression of the first two odd square wave harmonics is given by:

$$\frac{P_1}{P_T} = -3.92 \text{ dB, and}$$
$$\frac{P_2}{P_T} = -13.46 \text{ dB.}$$
(10)

3.2.4 DOR TONE SPACING RELATIVE TO CHANNEL ASSIGNMENT

Each deep-space mission is assigned a frequency channel to transmit on, from within the allocation for deep-space research. It should be noted that this use of the word ‘channel’ is distinct from the Δ DOR usage of channel to refer to a slice of the frequency spectrum to record. All spacecraft downlink signal components above a specified threshold should be within the allocation for deep-space research. If the assigned spacecraft frequency is near the edge of the allocation for deep-space research, there is a chance that a DOR tone will fall outside of the allocation. It may be necessary to request a waiver for such a transmission. With a modern transponder, an alternative would be to shape the downlink spectrum, using digital frequency synthesis, so that all signals are within band. It is still necessary to work through the Space Frequency Coordination Group (SFCG) to select downlink frequencies.

Phase modulation has been in widespread usage for deep-space transmitters. This can produce higher harmonics that may be valuable for Δ DOR purposes. But this also increases the possibility of interference with other missions or out-of-band signals. The use of vector modulation in modern transponders, in place of phase modulation, may reduce higher harmonics.

3.3 SPREAD SPECTRUM SIDEBANDS

3.3.1 RATIONALE FOR SPREAD SPECTRUM

One of the major error sources in a Δ DOR measurement is caused by the non-linear bandpass phase response in the ground station electronics. Receiving systems used for deep space communications are among the most sensitive and tightly specified radio systems in existence. Even so, phase linearity across channels of several MHz bandwidth, at the level of a fraction of a degree of phase, cannot be assumed. An illustration of how phase dispersion has a different effect on a broadband quasar signal versus a discrete DOR tone can be found in figure 3-1.

Phase dispersion of order 0.5 deg has been measured in modern digital recorders by observing strong quasars and extracting phase in narrow bins across the channel (reference [30]).

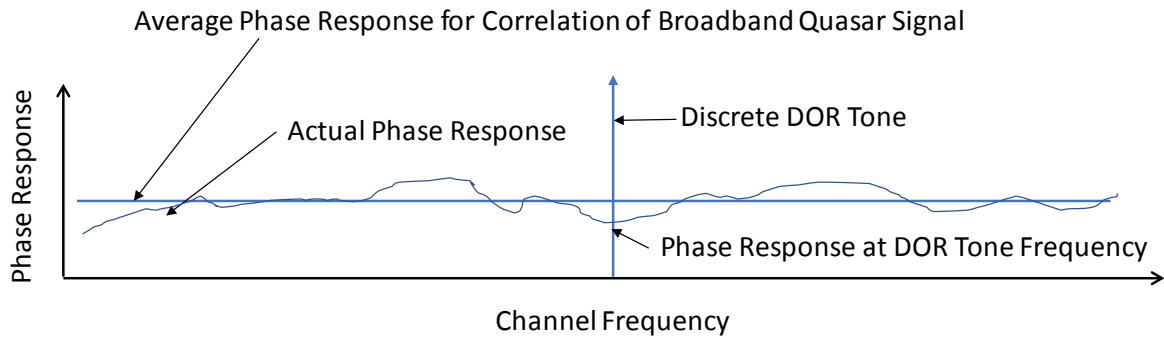
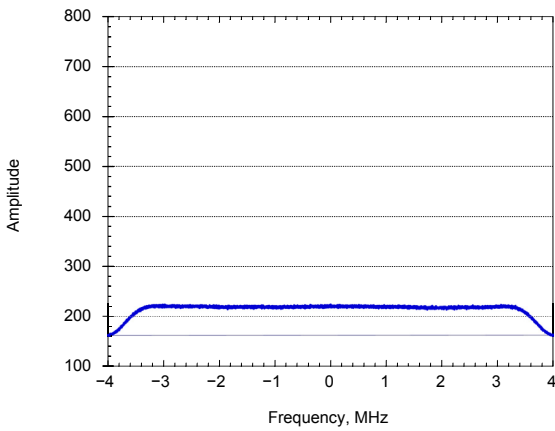


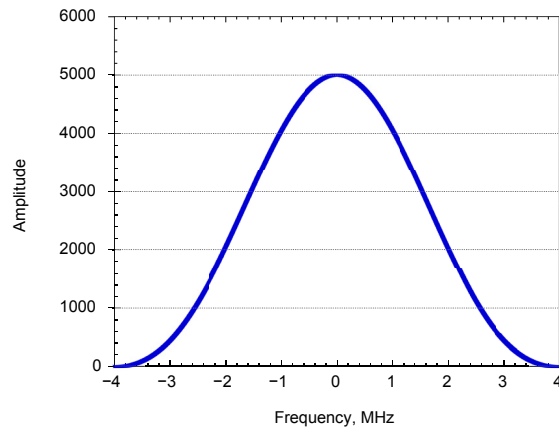
Figure 3-1: Illustration of Instrumental Error Due to Phase Dispersion within a Recording Channel

However, common-mode cancellation of phase dispersion effects is possible for Δ DOR by using a spread spectrum DOR signal. The basic idea is to make the spacecraft signal closely resemble the quasar white-noise signal. Consider figure 3-1. The two spectra on the left-hand side are data from an actual Δ DOR measurement. Figure 3-2a is the spectrum of receiver noise in a channel, with the quasar signal buried in the noise. Figure 3-2b is the spectrum of a spacecraft DOR tone in a noise channel. The two spectra on the right-hand side are theoretical spectra of a DOR tone spread with a PN code. Figure 3-2c is the spectrum of a PN code with rectangular chips. Figure 3-2d is the spectrum of a PN code with shaped chips.

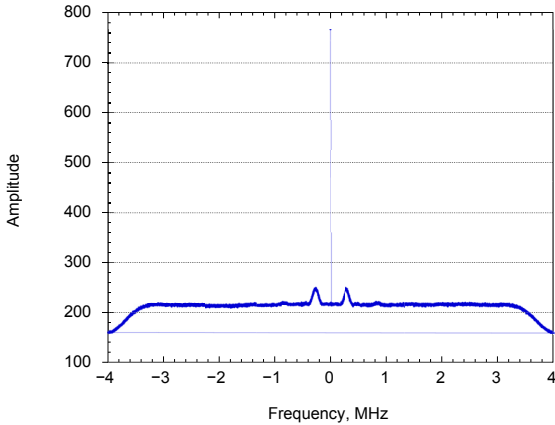
CCSDS REPORT CONCERNING DELTA-DOR—
TECHNICAL CHARACTERISTICS AND PERFORMANCE



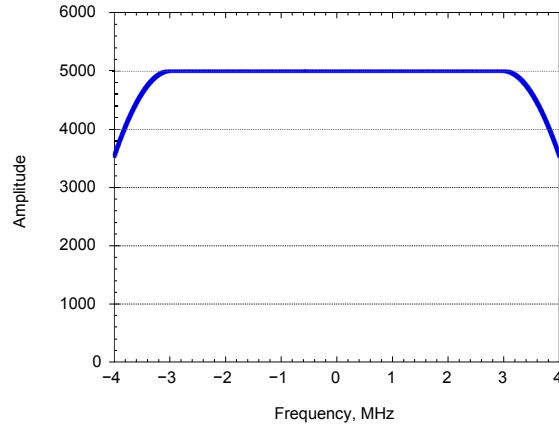
a. Quasar signal buried in noise channel



c. Theoretical PN code spectrum without shaping (no noise)



b. DOR tone in noise channel



d. Theoretical PN code spectrum with shaping (no noise)

Figure 3-2: Spectra of Quasar and Spacecraft DOR Signals

By choosing the PN-spreading code and shaping filter carefully, the spacecraft signal can closely resemble the quasar signal. If the DOR spectrum is spread across the channel bandwidth, then it is expected that the Δ DOR error due to phase dispersion will be reduced. Depending on ground station phase ripple performance and quality of the DOR spectrum spreading, this could be a reduction in phase-dispersion error of up to 90%. An ESA study carried out a mathematical simulation to evaluate the PN-spreading approach and confirmed its effectiveness (reference [31]). Larger error reduction requires the DOR spectrum to be flat over a larger fraction of the quasar recording bandwidth. The study showed several ways to achieve this. A consequence of spreading the DOR spectrum is that a higher data rate will be required to record the DOR signal as compared to a conventional sinusoidal signal.

The most accurate differential VLBI measurements of quasars do not carry a term for phase dispersion in their error budget (reference [29]). This effect, if any, is lower than that due to

tropospheric noise. Two signals, with the same spectra such as white noise, will see the same instrumental phase shift when passing through the same instrumentation. However, most differential VLBI and Δ DOR measurements observe sources sequentially rather than simultaneously, so the phase response of the front-end analog components may drift between source observations. It is unlikely that 100% error reduction can be achieved.

Like two-ray ranging, the code may be used for ambiguity resolution. A code period of 1 msec will resolve an ambiguity that is 1000 times greater than the 1 μ sec ambiguity that is provided by a 1 MHz sinusoidal DOR tone. The advantage to be able to resolve the Δ DOR ambiguity without a good a priori trajectory model is especially important for missions with dynamic-modelling problems, for example, constant ion propulsion, thruster leaks, or outgassing. It is also important for missions that have sparse tracking schedules, such as SmallSats, or for a mission coming out of hibernation.

Like two-way ranging, a local model of the code can be used in data processing, before station differencing, to recover the full signal without losing Signal-to-Noise Ratio (SNR) as would occur if cross-correlation were used for processing.

A secondary benefit of spread-spectrum modulation for DOR is that there will not be narrow-band DOR tones to interfere with other spacecraft downlinks or to exceed the flux-density threshold for out-of-band emissions.

3.3.2 PSEUDO NOISE SPREADING

A sinusoidal signal generated in a transponder for the purpose of DOR could be multiplied by a PN sequence before modulating the carrier. The PN code should be chosen to make the spacecraft signal similar to the quasar signal within the specified recording channel passband.

A suitable code could be generated with a Linear Feedback Shift Register (LFSR). A suitable code produced by a LFSR is called a maximum-length sequence or a shift-register sequence. This is a large family of codes, including the Gold codes.

The baseband power spectral density of one of these codes with rectangular chips is usually well approximated by a sinc-squared function, where $\text{sinc}(x) = \sin(\pi*x)/(\pi*x)$.

After this PN code multiplies a DOR subcarrier, the power spectral density of the composite signal would be a sinc-squared shape centered at the DOR subcarrier frequency with the main lobe occupying a bandwidth proportional to the chip rate. When the spread-spectrum DOR signal modulates the carrier, there will be a spread-spectrum signal on either side of the carrier, offset by the DOR subcarrier frequency.

Further, it is possible to get a composite signal that is closer to being white noise within the channel passband by using shaped chips, rather than rectangular chips. A Square Root Raised Cosine (SRRC) filter, such as used in CDMA applications, would be suitable for this purpose.

A long code sequence could be chosen to resolve the ambiguity within a single channel.

3.4 AMBIGUITY RESOLUTION

3.4.1 AMBIGUITY RESOLUTION USING SEQUENTIAL TONE SPACINGS

In Δ DOR processing, the quasar cross-correlation channel phases and the spacecraft station-differenced channel phases are the primary measured quantities. Only the fractional part of phase is measured, and the integer part must be determined from a priori knowledge. When multiple DOR channels are in the downlink spectrum, the closest spaced channels, that is, the channel pair with the smallest frequency separation BI , are initially used to resolve the integer cycle phase ambiguity. Refer to section 4 for equations that compute delay from measured phases.

The a priori knowledge of delay (spacecraft minus quasar) must be known to $1/(6BI)$, one-sigma, in order to resolve the ambiguity at the 99% level.

Next, the ambiguity can be resolved for a bandwidth of up to $(1/(6\alpha)) \times BI$, where α represents the interferometric measurement precision, one-sigma, in terms of fractions of a cycle. The only error terms that need be considered for sequential ambiguity resolution are thermal noise and instrumental phase dispersion (see 4.3.2). Values for α in Δ DOR applications normally fall in the range of 0.002 to 0.008 cycle, indicating that spanned bandwidth can be increased by a factor of 20 to 80 for successive tone pairs. The final measurement is based on the widest usable channel spacing.

3.4.2 AMBIGUITY RESOLUTION USING A SINGLE CHANNEL OF PN

Traditionally for Δ DOR, multiple channels are used to compute delay from phase by way of bandwidth synthesis. However, a single channel can be used if the signal has sufficiently wide bandwidth, such as a quasar signal in an 8 MHz channel, or a spacecraft PN code with a long code length. An unambiguous delay can be calculated for the quasar data, just by aligning the samples from the two stations to maximize correlation amplitude. This delay will be accurate to some fraction of the reciprocal channel bandwidth and may be adequate to resolve the ambiguity in the two closest-spaced frequency channels. Similarly, the spacecraft delay calculated from the longest single-channel code length may be adequate to resolve the ambiguity in the two closest-spaced frequency channels.

4 THEORETICAL BACKGROUND

4.1 MEASUREMENT EQUATIONS

4.1.1 VLBI

The technique of radio interferometry is well described in reference [1], including VLBI. In VLBI, signals from a distant radio source arrive at two widely separated receivers at slightly different times. The difference in time of arrival is measured to determine the angle between the baseline vector joining the two receivers and the direction to the radio source. The VLBI geometry is shown in figure 4-1, where the baseline vector \vec{B} goes from Receiver 1 to Receiver 2, and the direction to the radio source is \hat{s} . The delay from Receiver 1 to Receiver 2 is given approximately by

$$\tau \approx -\frac{1}{c} \vec{B} \cdot \hat{s} = -\frac{1}{c} B \cos \theta, \quad (11)$$

where B is the baseline length and θ is the angle between the baseline and the direction to the radio source.

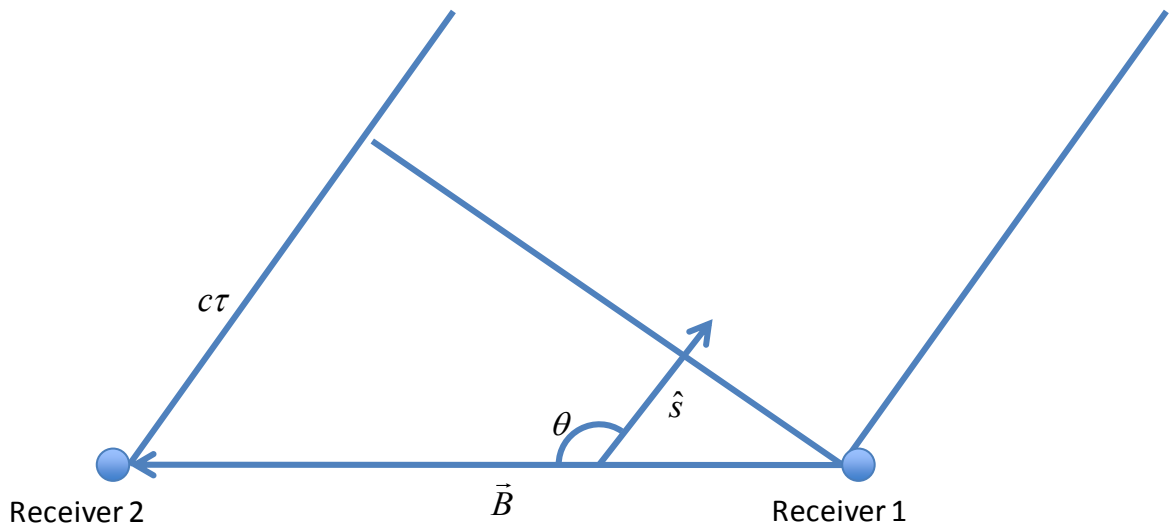


Figure 4-1: VLBI Geometry for Two Receivers and One Radio Source

4.1.2 DIFFERENTIAL VLBI

Since VLBI instruments are large systems, perhaps spanning continents, it is difficult to maintain system-level calibrations. For this reason, differential VLBI, in which two radio sources are observed and the angular offset between sources is measured, is a more useful data type for navigation purposes. The differential VLBI geometry is shown in figure 4-2, where the direction to the radio source 1 is \hat{s}_1 and the direction to the radio source 2 is \hat{s}_2 . The differential delay between source 1 and source 2 is given approximately by

$$\Delta\tau = \tau_1 - \tau_2 \approx -\frac{1}{c}\vec{B} \bullet (\hat{s}_1 - \hat{s}_2) \approx -\frac{1}{c}B \sin\theta_1(\theta_1 - \theta_2) = -\frac{1}{c}B \sin\theta_1(\Delta\theta_B), \quad (12)$$

where $\Delta\theta_B = \theta_1 - \theta_2$ is the component of the angular separation between the two radio sources that is in the direction of the baseline. Measurements along two independent baselines are needed to determine both components of angular position. The full angular separation between radio sources is denoted as $\Delta\theta$. The accuracy of the determination of $\Delta\theta_B$ from equation (12) improves as the measurement error in the observable $\Delta\tau$ decreases. Further, $\Delta\theta_B$ accuracy improves as the baseline length B increases. In addition, key terms in the error budget presented in 4.3 show that the accuracy in measurement of the observable $\Delta\tau$ improves as the spanned bandwidth f_{BW} increases (see equations (20), (23), and (25)), and $\Delta\tau$ accuracy improves as the angle $\Delta\theta$ between radio sources decreases (see equations (26) thru (30)). Combining these relations and taking partial derivatives provides an expression for the dependence of the accuracy of angular offset determination on the most important system parameters:

$$\sigma_{\Delta\theta_B} \propto \frac{\Delta\theta}{f_{BW}B}. \quad (13)$$

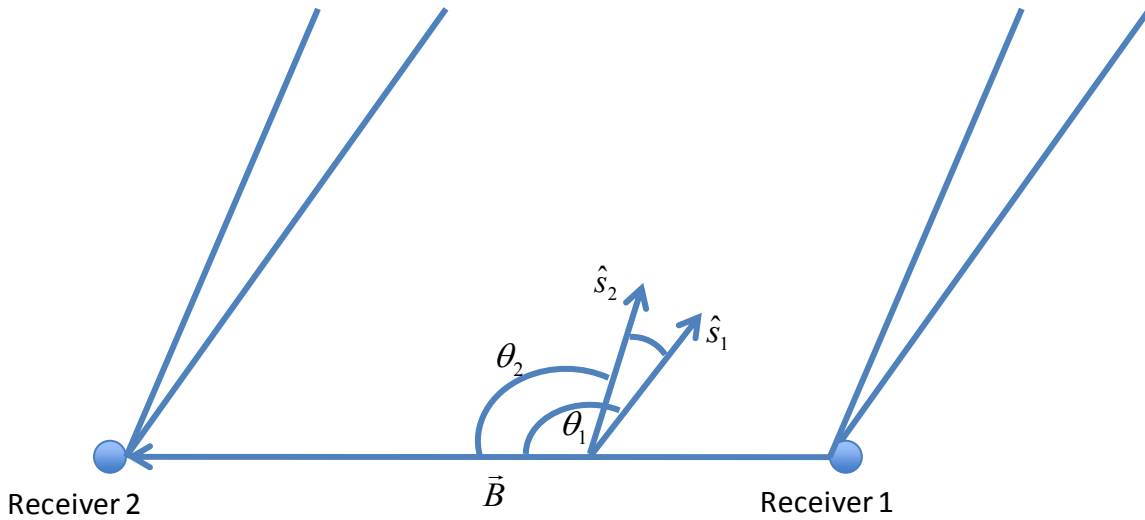


Figure 4-2: Differential VLBI Geometry for Two Receivers and Two Radio Sources

4.1.3 DELTA-DOR

4.1.3.1 General

Delta-DOR is a specific application of differential VLBI to spacecraft tracking. In Δ DOR, an interferometric measurement of a quasar with known coordinates (or an average of several quasar measurements) is subtracted from a differential range measurement of a spacecraft. Both of these measurement types are commonly referred to as delays. The measurement

system is configured so that these two types of observations will have nearly the same sensitivity to key error sources. The result of a Δ DOR measurement is knowledge of the spacecraft angular position in the inertial reference frame defined by the quasars.

Channels of the Radio Frequency (RF) spectrum are recorded during Delta-DOR observations. Channels are centered on the received frequencies of spacecraft tones. The channel sampling rate must be high enough to reduce thermal noise errors to an acceptable level (see equations (19) and (20)). An example is given in figure 4-3. The bandwidth-synthesis technique (reference [2]) is used to generate a group delay from phase measurements in each of several channels. The two outermost channels have the most strength to determine the delay observable. The frequency separation between the two outermost channels is referred to as the spanned bandwidth. Inner channels are used primarily to resolve the integer cycle phase ambiguity in the observed signals. The spacecraft delay is based on phase measurements of discrete tones in the downlink spectrum. Channels for recording quasar signals are centered on the received frequencies of the spacecraft tones.

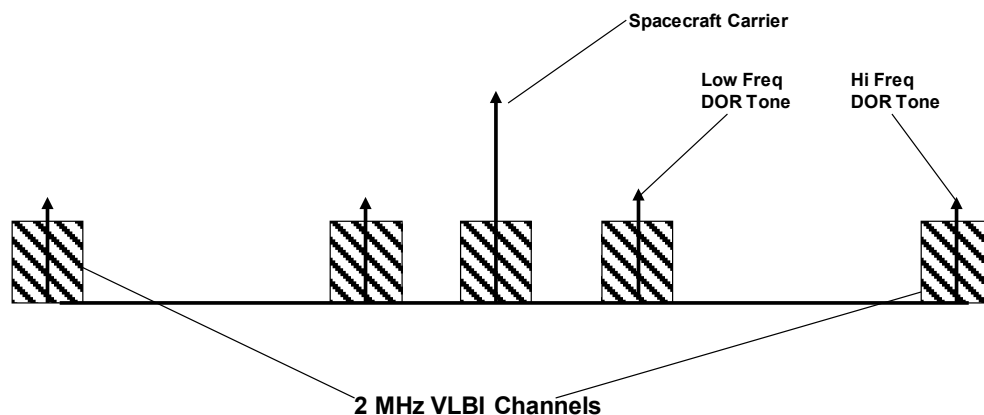


Figure 4-3: Downlink Tone Spectrum and Coincident VLBI Channels

4.1.3.2 Observable Modeling

In the navigation process, multiple Delta-DOR measurements are commonly combined with line-of-sight Doppler and range measurements to allow determination of three-dimensional spacecraft state. A model for the spacecraft trajectory (based on earlier information) must be available to start the processing of newly acquired data. The navigation process uses modeling to compare measured quantities with model values and then uses filtering to update the model so that it better agrees with the data. Measurements such as spacecraft delay are referred to as ‘observed’ observables. A model value for a measurement is based on the model spacecraft trajectory and existing models for other geometric and propagation parameters. A model value corresponding to a measurement is referred to as a ‘computed’ observable. The reader should refer to 2.4 of this document and to reference [7] for more information on the navigation process.

In navigation processing, to begin, each spacecraft and quasar measurement is processed individually. The observed observable depends on actual geometric factors and on actual delays introduced by transmission media. The computed observable is based on model values for geometric parameters and available calibrations for tropospheric and ionospheric delays. Meteorological data are normally provided from each tracking site so that, possibly in conjunction with other data such as GPS measurements, calibrations can be computed to account for tropospheric and ionospheric path delays. The observed observables for the spacecraft and quasar are defined by equations (6) and (8), respectively. The computed observables for the spacecraft and quasar are defined by equations (5) and (17), respectively.

Residuals are formed by subtracting the computed observables from the observed observables. For each Delta-DOR session, the ‘Delta’ between spacecraft and quasar observations is generated internal to the navigation processing by subtracting residual values of quasar observations from residual values of spacecraft observations. Normally, for a quasar-spacecraft-quasar sequence, quasar measurement residuals are interpolated to the time of a spacecraft measurement residual to form the Delta. Similarly, for a spacecraft-quasar-spacecraft sequence, spacecraft measurement residuals are interpolated to the time of a quasar measurement residual to form the Delta. Several distinct Delta-DOR residuals may be generated in this fashion from a tracking pass with multiple spacecraft and quasar observations. Alternatively, it is possible for navigation processing to estimate station clock epoch and rate parameters, and do implicit differencing using all separate time delays, rather than do explicit differencing.

The following subsections provide definitions of the spacecraft and quasar observables.

4.1.3.3 Computed Differential One-Way Range

The notation used in reference [3] is followed here. One-way range ρ_i (s) from a spacecraft to receiver i is defined as

$$\rho_i(t_3(ST)) = t_3(ST) - t_2(TAI) \text{ s}, \quad (14)$$

where $t_3(ST)$ is the time of signal arrival at the receiver as reported by the station clock and $t_2(TAI)$ is the time of signal emission as reported by an ideal atomic clock in the spacecraft rest frame. The time-tag for the measurement is $t_3(ST)$. The computed value of differential one-way range between receiver 1 and receiver 2 is defined as

$$\tau_{sc}^c = \Delta\rho(t_3(ST)) = \rho_2(t_3(ST)) - \rho_1(t_3(ST)) \text{ s}, \quad (15)$$

where ρ_2 is the one-way range at Station 2 at time $t_3(ST)$ as reported by the Station 2 clock and ρ_1 is the one-way range at Station 1 at the same time $t_3(ST)$ as reported by the Station 1 clock. The time-tag for the measurement is $t_3(ST)$. It should be noted that the superscript ‘C’ on the observable denotes this as the computed observable.

The spacecraft differential range is defined for signals received at the same time t_3 at each of two tracking stations. However, by combining equations (14) and (15), it can be shown that the spacecraft differential range is equal to the delay δt_2 in transmission time, in the spacecraft rest frame, for the signals that arrive at the two stations at common time t_3 . Hence the spacecraft differential range is commonly referred to as a time delay.

NOTE – Measurements of differential range between receivers can also be made if the ranging signal is uplinked from a transmitter and then transponded by a spacecraft (reference [3]). In this case, one-way range is replaced by round-trip range in the definition.

4.1.3.4 Observed Differential One-Way Range

The phase of a received spacecraft tone is measured, relative to the phase of the station clock. There are several downconversion steps, from RF to baseband, before the measurement is made. A model of the downconverter phase is restored by the processing software, so that the measurement may be considered to be a measurement of RF phase. A spacecraft tone phase measurement is made for each of the two stations. The phase is measured at a common Earth receive time, as read from the local clock at each station, of $t_3(ST)$. The signals received at the two stations at time $t_3(ST)$ will in general have been transmitted at different times by the spacecraft. This convention distinguishes spacecraft differential range measurements from the interferometric delay observable used for quasars.

A spacecraft phase measurement is made for each of two tones in the downlink spectrum, and for each of two stations, at common Earth receive time $t_3(ST)$. With ϕ_j^i denoting the measured phase, for tone j , at station i , an estimate is made of the transmitter frequency at the time of signal transmission. If the measurement is of type one-way (DOR tones from onboard oscillator or harmonics of independent subcarrier), then the onboard oscillator (or subcarrier) frequency is estimated, in the spacecraft rest frame, as one-way light time before $t_3(ST)$. (The actual time used is the average of the spacecraft transmit times for the two stations.) One-way Doppler collected by the station at the time of the measurement is used with existing spacecraft trajectory predicts to make this estimate. The estimated transmitter frequency for tone j is denoted as f_j . Next, the observed value of differential range, also known as delay, is calculated as

$$\tau_{SC}^O = \frac{(\phi_2^1 - \phi_2^2) - (\phi_1^1 - \phi_1^2)}{f_2 - f_1} \text{ s.} \quad (16)$$

Given that phase has units of cycles, and frequency has units of Hz, the delay has units of seconds. The time-tag for the measurement is $t_3(ST)$. It should be noted that the superscript ‘O’ on the observable denotes this as the observed observable. The deviation of Station Time from Universal Time Coordinated (UTC) and an instrumental delay from the station front end electronics to the recorder system are modeled separately for each station.

The spacecraft delay is defined using this convention for two reasons. First, measurement of the phase of discrete components in the spacecraft downlink spectrum, locally at each station, is more efficient and more precise than cross-correlation. Second, integer cycle phase ambiguities may be resolved in an analogous manner to resolution of spacecraft range code ambiguities.

If the measurement is of type 2-way (DOR tones coherent with an uplink or uplinked range tones), then the meaning of f_j changes. Now f_j is the ground transmitter frequency at the uplink station, for tone j , at a round-trip light time prior to $t_3(ST)$. (The actual time used is the average of the ground transmit times for the two stations.) No estimate is needed here, except for the round-trip light time. The actual transmitter frequency at the uplink station is used. A scale factor is applied to the RF transmitter frequency to get the tone component frequency. The meaning of ϕ_j^i does not change. Equation (16) is used again to compute observed delay from phase. Equation (16) is the same as equation (13-132) in reference [3].

4.1.3.5 Computed Quasar Interferometric Delay

The notation used in reference [3] is followed here. A natural radio source emits a signal and a wavefront propagates towards two receivers. The signal wavefront arrives at Receiver 1 at time $t_3(ST_1)$ as reported by the Station 1 clock. The same signal wavefront arrives at Receiver 2 at time $t_3(ST_2)$ as reported by the Station 2 clock. Computed interferometric delay from Receiver 1 to Receiver 2 is defined as

$$\tau_{QU}^C = t_3(ST_2) - t_3(ST_1) \text{ s,} \quad (17)$$

with time-tag $t_3(ST_i)$. This definition is not symmetric with respect to station order, but is conventional in astrometric and geodetic applications (reference [4]).

4.1.3.6 Observed Quasar Interferometric Delay

Quasar signals received at two stations are mixed together (i.e., cross-correlated) to produce a beat note that has an amplitude and phase that can be measured. To get a non-zero output, it is necessary at the time of signal processing to align the signals from the two stations so that one station is delayed relative to the other station by an amount that corresponds to the actual difference in signal arrival times. By convention, the measurement time-tag is the reception time at Station 1. The Station 2 bit stream is delayed by an amount such that the wavefront recorded at Station 1 at the time-tag is mixed with the same wavefront recorded at Station 2 at the time-tag plus the delay. Delay may be either positive or negative in this application, depending on the geometry. For a 1 MHz channel sample rate, the delay model used at the correlator must be correct to about 1 μ s to get valid output from the interferometer. In general, the bit streams must be aligned with an accuracy that is the inverse of the channel bandwidth. The observable, however, is not this crude delay, but rather the phase of the beat note. It can be shown that this phase is a function of the true wavefront travel time from Station 1 to Station 2 and of the channel reference frequency.

Phase can be measured for one or more frequency channels that are downconverted and filtered slices of the received broadband RF signal. The measured phase is denoted as ϕ_j for channel j . The reference frequency \bar{f}_j for channel j is the weighted center of the received frequency slice, and is a function of the downconverter frequencies at the two stations and of the filter characteristics. All downconverter phases and model terms are restored, so that the interferometric phase may be considered to be an RF measurement.

Interferometric phase ϕ_j is measured in each of two channels, at time $t_3(ST)$ at Station 1. Observed delay is calculated from the observed phases as

$$\tau_{\text{QU}}^o = \frac{\phi_2 - \phi_1}{f_2 - f_1} \text{ s.} \quad (18)$$

Given that phase has units of cycles, and frequency has units of Hz, the delay has units of seconds. The time-tag is $t_3(ST)$. Equation (18) is the same as equations (13-168) in reference [3]. Equation (18) is also consistent with equation (10) in section 11 of reference [4]. As noted in section 11 of reference [4], the convention for VLBI delay observables is that the measurement time scale is defined by the station clocks (i.e., terrestrial time, realized as UTC) and is not scaled to Geocentric Coordinate Time. Reference [1] provides additional background information about radio interferometry.

Just as for spacecraft delay, the deviation of Station Time from UTC and an instrumental delay from the station front end electronics to the recorder system are modeled separately for each station.

4.2 DELTA-DOR AS A NAVIGATION TECHNIQUE

Delta-DOR measurements are a source of data that may be used in the spacecraft navigation process. The CCSDS Navigation Green Book (reference [7]) describes the navigation process in general. A single Delta-DOR measurement provides one component of spacecraft state, namely the component of angular position in the direction of the baseline projected onto the plane-of-sky; the projection is along the line of sight from the baseline to the radio source. Measurements on two independent baselines determine both coordinates of angular position. Several Δ DOR measurements over a time arc, usually spanning days to weeks, determine the rate of change of angular components.

Normally, not all components of spacecraft state may be measured at the same time. Data, including Doppler, range, Δ DOR, and possibly other types of measurements, are acquired and used together to solve for a spacecraft ephemeris. The ephemeris could span the arc of the collected data and be propagated forwards and/or backwards by applying known force models and the laws of motion. In addition to being part of the data mix used to estimate a spacecraft trajectory, the Δ DOR data also provide an estimate of trajectory error. Since Δ DOR is a direct geometric measure of plane-of-sky spacecraft position, the residual, that is, observed value minus computed value based on an ephemeris, is a direct measure of the

ephemeris error. The availability of range data combined with Δ DOR from two baselines provides full three-dimensional observability for spacecraft state.

Computation of the uncertainty associated with a spacecraft ephemeris is an important output of the navigation process. Since Δ DOR may be the strongest data type that is used to estimate the ephemeris, it follows that it is important to correctly characterize the uncertainties, both random and systematic, associated with Δ DOR measurements. A random error is associated with each data point. Systematic errors are better represented using a model and parameters to characterize the effect causing the error.

4.3 THE DELTA-DOR ERROR BUDGET

4.3.1 GENERAL

Modeling of Delta-DOR measurement errors is usually broken into random and systematic components to allow for statistically correct representations of solution uncertainty. Random components are root-sum-squared together to provide a single error bar for each Delta-DOR observable. Systematic components should be individually modeled in the navigation software. Both random errors and systematic errors are presented in this section. The systematic errors are generally more dependent on actual geometry; the effects of modeled systematic errors are properly determined in the navigation software. Here, an estimate is given for the magnitude of systematic errors, just for informational and comparison purposes.

The Delta-DOR error budget depends on a number of factors, including:

- a) observation geometry;
- b) signal RF;
- c) signal spanned bandwidth;
- d) spacecraft DOR tone SNR;
- e) quasar SNR;
- f) uncertainty in the quasar position coordinates;
- g) clock instability;
- h) instrumental phase ripple;
- i) uncertainty in station location coordinates;
- j) uncertainty in the orientation of the Earth in inertial space;
- k) uncertainty in the tropospheric delay;
- l) uncertainty in the ionospheric delay; and
- m) solar plasma induced delay error.

Parameters necessary to define these factors and to characterize the measurement error are given in this section. Equations providing sensitivity of measured delay to these factors are also given. Then, the predicted Delta-DOR measurement accuracy can be computed as the Root Sum Square (RSS) of terms derived from knowledge of these parameters and from the sensitivity equations. It should be noted that the error budget is for the difference in the spacecraft and quasar delay rather than for single source delay. As will be seen, some of the equations are empirical rather than derived from first principles. Radio wave propagation and VLBI are understood well enough to allow first principles derivations of all major effects, but these derivations generally contain unknown scale factors that depend, for example, on weather conditions. The empirical equations given here are based on analysis of data and are good enough to describe the typical uses of this data type.

As some parameters are used in the calculation of several different error budget components, they are defined only for the first use. All parameters are provided in table 4-1 for reference. All delay errors are given in units of seconds at the one sigma level.

4.3.2 COMPONENTS OF THE DELTA-DOR ERROR BUDGET

Observation Scenario: The scenario described here is based on spacecraft tracking at X-band and current system architecture.

Two widely separated stations simultaneously observe a spacecraft and, a short time before or after, one or more reference sources during a Δ DOR measurement. The pass typically takes about one hour, and the antennas slew between spacecraft and quasar several times. For each pass, sources should be selected and observing times chosen, to provide the best geometry within constraints. Sources are selected that are angularly close to the spacecraft. Observing times close to the station overlap center are preferred to maximize the station elevation viewing angles. A typical pass consists of six spacecraft and quasar scans in sequence Q1-S-Q2-Q1-S-Q2. The first quasar is usually offset to one side (i.e., lower right ascension) of the spacecraft, while the second quasar is offset to the opposite side. An ideal geometry has the spacecraft angular location midway between the two quasars. The Δ DOR observation is designed to completely cancel all first-order temporal and spatial errors for this case. If the spacecraft is within about 6 deg of one quasar, then this one quasar may be used for all quasar scans. Otherwise, the quasar catalog is dense enough so that, usually, two quasars may be selected that provide an ‘effective average quasar’, located midway on the arc joining the two actual sources, that is within about 6 deg of the spacecraft.

The following parameters characterize the observing geometry and schedule. The parameter values are for one spacecraft-quasar sequence such as Q1-S-Q2. The abbreviations SC and QU are used for spacecraft and quasar related parameters, respectively. Angles are based on the ‘effective average quasar’ location in case two different quasars are observed.

- total quasar observation time T_{QU} , s;
- total spacecraft observation time T_{SC} , s;

CCSDS REPORT CONCERNING DELTA-DOR—
TECHNICAL CHARACTERISTICS AND PERFORMANCE

- angular separation between SC and QU $\Delta\theta$, rad;
- spacecraft elevation angle at station i γ_{sc_i} , deg;
- quasar elevation angle at station i γ_{QU_i} , deg;
- minimum angle between Sun and SC or QU SEP , deg.

The error budget assumes that scan times are chosen long enough (at least a few minutes each) to reduce errors due to the shorter temporal period media fluctuations to acceptable levels. Enough slews between spacecraft and quasar are assumed to reduce errors due to the longer temporal period media fluctuations to acceptable levels.

Spanned Bandwidth: The maximum separation between spectral components in the spacecraft downlink is an important parameter in the Δ DOR error budget. In Δ DOR, group delays are synthesized from phase measurements made in separated frequency channels. Measured phases are subtracted between channels and divided by the spanned bandwidth to generate delay. For a given level of phase measurement error, the delay error scales down as spanned bandwidth increases. The spanned bandwidth parameter is:

$$\text{spanned bandwidth} \quad f_{BW}, \text{ Hz.}$$

The same value of spanned bandwidth is assumed for all spacecraft and quasar observations. The quasar channels are aligned with the spacecraft channels to achieve the best cancellation of instrumental effects.

Quasar Thermal Noise (Random): The delay error depends on the ratio of antenna gain to system noise temperature (G/T) of the receiving antennas, source flux, channel sampling rate, observation time, and spanned bandwidth. Depending on the antennas that are allocated for a pass, and the flux of the selected quasar(s), the channel sampling rate should be chosen to reduce this error term to an acceptable level while not increasing the data volume beyond practical limits. It is understood that when multiple spacecraft must be supported with quick turnaround, then the highest sampling rate cannot be used for all passes.

Channel bandwidths of 1, 2, and 4 MHz have been used, with resolution of 2 bits/sample. The corresponding sampling rates are 2, 4, and 8 megasamples/s per channel. At least two channels must be recorded to form a group delay. Additional channels are recorded for ambiguity resolution, but fewer bits need be returned for these ‘inner’ channels. Measurement precision for inner channels need only be good enough to resolve the integer-cycle ambiguity in the outer channels. The parameters that affect this error term include:

- G/T for antenna i $(G/T)_i$, K^{-1} ;
- channel sampling rate D , samples/s;
- quasar correlated flux (unpolarized) S_c , Jy;

CCSDS REPORT CONCERNING DELTA-DOR—
TECHNICAL CHARACTERISTICS AND PERFORMANCE

- system loss factor¹ K_L ;
- Boltzman constant $k=1.38 \times 10^{-23}$ Joules/K;
- RF wavelength λ , m.

After correlation of recorded data between two stations, averaging over the duration T_{QU} , assuming the recording is at a single polarization, and without consideration for sample quantization, the voltage SNR for a single channel of data is given by

$$SNR_{QU} = K_L \frac{10^{-26}}{2k} \frac{\lambda^2}{4\pi} S_c \sqrt{(G/T)_1 (G/T)_2} \sqrt{DT_{QU}}. \quad (19)$$

Sample quantization causes some loss of SNR, as discussed in 8.3 of reference [1]. The loss is about 2 dB for 1-bit samples and about ½ dB for 2-bit samples. Normally, 2-bit samples are used.

When delay is calculated from phase measurements in two channels separated by f_{BW} , the delay error is given by

$$\epsilon_{\tau_{QU}} = \frac{\sqrt{2}}{2\pi f_{BW}} \frac{1}{SNR_{QU}} \text{ s}. \quad (20)$$

Spacecraft Thermal Noise (Random): The delay error depends on received signal-to-noise spectral density of the DOR tone (P_{DOR}/N_0), observation time, and spanned bandwidth. These parameters are used in the calculations:

- effective transmitted tone power along line-of-sight to receiver P_{tran} , Watts;
- distance from spacecraft to receiver R , m;
- received tone flux FL , Watts/m².

The received tone signal-to-noise spectral density, at station i , is given by

$$(P_{DOR} / N_0)_i = P_{tran} \left(\frac{\lambda}{4\pi R} \right)^2 \frac{1}{k} (G/T)_i. \quad (21)$$

The ratio P_{DOR}/N_0 can also be determined from received spacecraft tone flux (power per unit area). Flux (FL) is related to effective transmitter power and distance by

$$FL = P_{tran} \left(\frac{\lambda}{4\pi R} \right)^2 \frac{4\pi(1m)^2}{\lambda^2}. \quad (21a)$$

¹ This parameter is system dependent and may vary from implementation to implementation.

Substituting flux into equation (21) provides the relation between P_{DOR}/N_0 , at station i , and flux

$$\left(P_{DOR} / N_0\right)_i = FL \left(\frac{\lambda^2}{4\pi(1m)^2} \right) \frac{1}{k} (G / T)_i. \quad (21b)$$

After tone phase extraction, and averaging over the duration T_{SC} , the voltage SNR for a single tone at station i is given by

$$SNR_{SC_i} = \sqrt{2(P_{DOR} / N_0)_i T_{SC}}. \quad (22)$$

The delay is generated from two tones at each of two stations, and the delay error is given by

$$\varepsilon_{\tau_{SC}} = \left[\left(\frac{\sqrt{2}}{2\pi f_{BW}} \frac{1}{SNR_{SC_1}} \right)^2 + \left(\frac{\sqrt{2}}{2\pi f_{BW}} \frac{1}{SNR_{SC_2}} \right)^2 \right]^{1/2} \text{ s}. \quad (23)$$

This expression assumes that the two tones at a given station have the same signal level. If this is not the case, then a separate term (without the $\sqrt{2}$ in the numerator) should be root-sum-squared for each tone.

Clock Instability (Random): The delay error depends on non-linear variations of the ground station frequency standard (or frequency distribution system), at each station, over the interval between the centers of adjacent spacecraft and quasar observations. These parameters are used:

- time between SC and QU observations T_{SC-QU} , s;
- instrument frequency stability ε_{Aff} .

The delay error is given by

$$\varepsilon_{\Delta\tau} = T_{SC-QU} \varepsilon_{Aff} \text{ s}. \quad (24)$$

Dispersive Phase (Random):² The delay error depends on the difference in the instrumental phase shift between the spacecraft and quasar signals, and on the spanned bandwidth. The quasar signal is broadband and is affected by the average instrumental phase delay over the few-megahertz channel width. The spacecraft signal is narrowband and is affected by the local instrumental phase delay at the received frequency of the spacecraft tone. The linearity of the receiving system over the channel bandwidth is the important parameter. An independent phase error occurs in each channel, but linearity over the full spanned bandwidth is not required. This instrumental phase error is referred to as dispersive phase or phase

² The dispersive phase-error estimate given here is for sinusoidal DOR tones. (See 5.3 and 5.4 for revised error estimates for spread spectrum DOR signals.)

ripple, and is represented by a deviation of the instantaneous phase response from the average smooth phase response over the channel.

Front-end components are broadband and have relatively little dispersion over channels as narrow as a few megahertz. A good instrument design is to digitize the signal over the full bandwidth, near the front end, and then use digital filters with linear phase response for all baseband processing. Narrowband analog filters should be avoided. The parameter that is used for this term is:

instrument phase ripple ε_{ϕ} , deg.

The phase error is assumed to be independent at each station and for each channel. The delay error is given by

$$\varepsilon_{\Delta\tau} = \sqrt{2}\sqrt{2} \frac{\varepsilon_{\phi}}{360} \frac{1}{f_{BW}} \text{ s.} \quad (25)$$

If the stations are known to have different values for phase ripple, then the error should be calculated as the root-sum-square of separate terms.

Station Location (Systematic): The delay error depends on the error in the baseline vector projected onto the direction of the angular separation between the spacecraft and quasar. The error scales with the magnitude of the angular separation between the spacecraft and quasar. The parameter that is used for this term is:

baseline coordinate uncertainty, each component ε_{BL} , m.

The delay error is given by

$$\varepsilon_{\Delta\tau} = \frac{1}{c} (\Delta\theta) \varepsilon_{BL} \text{ s.} \quad (26)$$

It should be noted that while the measurement for a baseline \bar{B} is sensitive to the component of source angular separation in the direction of the projection of \bar{B} , the error in the measurement is sensitive to the component of source angular separation in the direction of the projection of the vector representing the baseline error.

Earth Orientation (Systematic): The delay error depends on the accuracy of model parameters used to rotate the crust of the Earth into inertial space, and it scales with the magnitude of the angular separation between the spacecraft and quasar. These Earth-orientation parameters are referred to as Universal Time number 1 (UT1) and polar motion. VLBI measurements of distant radio sources are needed to make an absolute determination of UT1, while GPS satellite observations determine changes in UT1 and polar motion. Accordingly, these parameters are determined with high accuracy after the fact, but predicted values must be used for real-time spacecraft orbit solutions. Predictive errors in Earth orientation are usually dominated by UT1. The parameter that is used for this term is:

Earth orientation uncertainty, each component ε_{UTPM} , m.

The delay error is given by

$$\varepsilon_{\Delta\tau} = \frac{1}{c}(\Delta\theta)\varepsilon_{UTPM} \text{ s.} \quad (27)$$

For data that are re-analyzed after the fact, this error term drops to a very small value.

Zenith Troposphere (Systematic): Meteorological data from each site, supplemented when possible with GPS satellite observations and/or water vapor radiometer data, are used to generate calibrations for zenith troposphere delay. The Δ DOR delay error depends on the accuracy of the zenith troposphere calibration, the elevation angle, and the difference in elevation angles between spacecraft and quasar. The delay error scales as the inverse of sine of elevation. The key to keeping the Δ DOR error small is to observe at high elevation angles. The parameters that are used for this term are:

- zenith wet troposphere delay uncertainty at station i $\rho_{z_{wet_i}}$, m;
- zenith dry troposphere delay uncertainty at station i $\rho_{z_{dry_i}}$, m.

There is a delay error term for each station and for both wet and dry components. All error terms have the form

$$\varepsilon_{\Delta\tau} = \frac{\rho_z}{c} \left| \frac{1}{\sin \gamma_{SC} + 0.015} - \frac{1}{\sin \gamma_{QU} + 0.015} \right| \text{ s.} \quad (28)$$

The four error terms should be root-sum-squared to get an estimate of the total systematic troposphere error. A more precise mapping function could be used for an error estimate, but the simple mapping function given here is adequate for error estimation for the range of elevation angles typically observed.

Fluctuating Troposphere (Random): The actual tropospheric delay along a particular line-of-sight will have both temporal and spatial variations relative to the model represented by the zenith delay and mapping function. The Δ DOR error depends on the portion of this delay that does not cancel after differencing between spacecraft and quasar. This in turn depends on elevation angle and angular separation. Estimates for this error can be derived from analysis of the scatter in VLBI residuals for large data sets dominated by troposphere error, or from calculations involving structure functions that were derived from some measure of troposphere fluctuations. Here an empirical expression is given; the delay error for an angular separation of 10 deg is taken as an input parameter, based on prior data analyses:

fluctuating troposphere uncertainty for 10 deg separation $\rho_{\text{tropfluct}}$, m.

The delay error is then calculated by linearly scaling this term to the actual angular separation:

$$\varepsilon_{\Delta\tau} = \frac{1}{c} \left(\frac{\Delta\theta}{0.1745} \right) \rho_{trop_{fluct}} \text{ s.} \quad (29)$$

The key to keeping the ΔDOR error small is to observe at high elevation angles, keep the angular separation small, and slew between sources several times.

Ionosphere Shell (Systematic): Global maps of ionospheric delay are derived from dual frequency GPS satellite measurements from receivers all over the world. Calibration accuracy for a particular station is better when there are receivers at and surrounding the station. The ΔDOR error depends on the error in the calibration value that does not cancel between the spacecraft and quasar. For error-modeling purposes, it is convenient to use partial derivatives of the ionosphere shell model of Klobuchar (references [8] and [3]). A nighttime value and a peak daytime value for zenith ionosphere delay uncertainty are specified. The parameters are:

- daytime ionosphere model uncertainty (X-band level) at station i $\rho_{iono_{day_i}}$, m;
- nighttime ionosphere model uncertainty (X-band level) at station i $\rho_{iono_{night_i}}$, m.

The Klobuchar model scales the line-of-sight error estimate as a function of where the raypath pierces the ionospheric shell in relation to the local ionospheric bulge, and also as a function of elevation. The differential delay error depends on the angular separation between sources. Typical values for daytime and nighttime delay error (see table 4-1) yield a differential delay error estimate of 0.02 ns for daytime measurements that follow the observation assumptions. For rough error estimation purposes, it is permissible to use equation (30) defined below to estimate this term, rather than the Klobuchar model.

Fluctuating Ionosphere (Random): An empirical model is used to estimate the ΔDOR error due to temporal and spatial variations in the ionosphere that are not represented by the model of Klobuchar. Just as for the fluctuating troposphere, the delay error for an angular separation of 10 deg is taken as an input parameter, based on prior data analyses.

$$\text{fluctuating ionosphere uncertainty for 10 deg separation} \quad \rho_{iono_{fluct}}, \text{ m}$$

The delay error is then calculated by linearly scaling this term to the actual angular separation:

$$\varepsilon_{\Delta\tau} = \frac{1}{c} \left(\frac{\Delta\theta}{0.1745} \right) \rho_{iono_{fluct}} \text{ s.} \quad (30)$$

It should be recognized that there can be anomalies in the ionosphere that result in much larger variations and hence much larger ΔDOR errors. Also, the magnitude of this effect is larger by about a factor of two for solar maximum, as compared to solar minimum.

Solar Plasma (Random): The effects of solar plasma mostly cancel between the two stations involved in a VLBI measurement. At X-band, the error is not significant outside of about 10

deg Sun-Earth-Probe (SEP) angle, that is, for raypaths that are separated by more than 10 deg from the Sun. The solar plasma error depends on signal frequency and proximity of the signal raypaths to the sun. An estimate for the delay error is given by Callahan (reference [9]). The parameters in addition to SEP used in the estimate are:

- signal RF f_{RF} , GHz;
- raypath separation at plane of signal closest approach to Sun B_s , m;
- solar wind velocity v_{SW} , m/s.

The delay error is given by

$$\varepsilon_\tau = \frac{0.013}{f_{RF}^2} [\sin(SEP)]^{-1.3} \left(\frac{B_s}{v_{SW}} \right)^{0.75} \times 10^{-9} \text{ s.} \quad (31)$$

There is a term of this form for both the spacecraft and the quasar. Cancellation of this effect between radio sources will not occur unless the raypaths for the different sources are at separations comparable to the baseline length, such as for two radio sources within the same antenna beamwidth.

Quasar Coordinate (Systematic): The quasars selected for use as Δ DOR reference sources have positions that are known in the *International Celestial Reference Frame* (reference [10]). Most of the catalog sources have position accuracy in the range of 0.5 to 2.0 nrad. For Δ DOR, it is a priority to select sources from the catalog that have less structure effects and better-known positions. The parameters used for this term are:

- quasar coordinate uncertainty ε_g , rad;
- length of baseline projection onto plane-of-sky B_p , m.

Assuming a spherical coordinate uncertainty, the delay error is given by

$$\varepsilon_{\tau_{QU}} = \frac{B_p}{c} \varepsilon_g \text{ s.} \quad (32)$$

4.3.3 DELTA-DOR ERROR ESTIMATES

To estimate Δ DOR errors, nominal values for all parameters must be assigned, and assumptions about measurement geometry must be made. Table 4-1 provides nominal values for all parameters that are representative of current NASA system capabilities. When estimating performance for other networks, these assumptions should be reviewed and revised as appropriate. The models of the previous subsections of this document are used to compute error terms from the parameter values. A total expected error is then computed as the root-sum-square of the terms. Table 4-2 lists the measurement errors by components.

This table includes both random and systematic effects. The error budget is plotted in figure 4-4.

In addition to computing the expected total error, the components of the error budget are broken into random and systematic components. This breakdown is useful for covariance analyses. The actual geometry is then used to compute individual systematic errors, and correlations between measurements are properly accounted for. Table 4-3 lists the random components of the error budget. The RSS total at the bottom of table 4-2 would be the recommended data weight for a single Δ DOR measurement, provided the nominal parameter values in table 4-1 properly characterize the measurement and calibration systems. Systematic error sources are listed in table 4-4. When using the data weight from table 4-2, the effects of the error sources in table 4-4 should be explicitly accounted for in the navigation modeling to develop a realistic covariance for orbit solutions that incorporate Δ DOR measurements.

All errors are listed at the one-sigma level. Measurement errors in these tables and figures are given in units of nanoseconds of time delay. The error may be converted from units of time delay to units of angle by multiplying by the speed of light and dividing by the length of the baseline projected onto the plane-of-the-sky. The angular error may then be converted into a position error at the spacecraft, normal to the line of sight, by multiplying by the Earth-spacecraft distance.

4.3.4 DELTA-DOR ERROR BUDGET SUMMARY – CURRENT CAPABILITY

Precision and accuracy: Precision refers to the statistical error in the measurement based on empirical scatter in the data. Accuracy refers to the difference between the measurement and truth. The precision of a spacecraft DOR measurement depends on the received tone power-to-noise power ratio and on the spanned bandwidth of the DOR tones. But the accuracy of a Delta-DOR measurement also depends on the precision of the quasar delay measurement, on knowledge of the quasar position, on clock stability, on instrumental phase response, and on uncertainties in Earth platform models and transmission media delays. Space missions typically utilize Delta-DOR to meet certain navigation requirements. Requirements or guidelines for interagency Delta-DOR accuracy should be specified in an Implementing Arrangement (reference [34]). Then, a strategy to provide the required accuracy for model parameters (quasar coordinate, station location, transmission media delay, Earth orientation) and observed delays should be developed.

Table 4-1: Nominal Parameter Values [Typical NASA Case] for Evaluation of Δ DOR Error Budget

Term	Description	Nominal Value
T_{QU}	Total quasar observation time	960 s
T_{SC}	Total spacecraft observation time	480 s
$\Delta\theta$	Angular separation between spacecraft and quasar	0.1 rad

CCSDS REPORT CONCERNING DELTA-DOR—
TECHNICAL CHARACTERISTICS AND PERFORMANCE

Term	Description	Nominal Value
$\Delta\theta_B$	Component of spacecraft-quasar angular separation in direction of baseline projection	0.1 rad
γ_{SC_i}	Spacecraft elevation angle at station i	20 deg
γ_{QU_i}	Quasar elevation angle at station i	25 deg
SEP	Minimum angle between Sun and spacecraft or quasar	20 deg
f_{BW}	Spanned bandwidth	38.25×10^6 Hz
$(G/T)_i$	G/T for antenna i	52.56 dB K ⁻¹
D	Channel sampling rate	16×10^6 samples/s
S_c	Quasar correlated flux density	0.4 Jy
K_L	System loss factor	0.8
k	Boltzman constant	1.38×10^{-23} Joules/K
λ	RF wavelength	0.0356 m
SNR_{QU}	Quasar voltage SNR (derived)	261
P_{tran}	Effective transmitted tone power	108 Watts
R	Distance from spacecraft to receiver	150×10^9 m
FL	Spacecraft tone flux (derived)	3.981×10^{-22} W/m ²
$(P_{DOR}/N_0)_i$	DOR tone power to noise spectral density, station i (derived)	27 dB•Hz
SNR_{SC_i}	Spacecraft voltage SNR (derived)	695
T_{SC-QU}	Time between centers of spacecraft and quasar scans	600 s
ϵ_{Aff}	Instrument frequency stability at 600 s	10^{-14}
ϵ_ϕ	Instrument phase ripple (nonlinearity across channel of few MHz bandwidth)	0.2 deg
ϵ_{BL}	Baseline coordinate uncertainty, each component	0.02 m
ϵ_{UTPM}	Baseline orientation uncertainty, each component (1 day prediction)	0.02 m
$\rho_{z_{wet}_i}$	Zenith wet troposphere delay uncertainty, station i	0.005 m
$\rho_{z_{dry}_i}$	Zenith dry troposphere delay uncertainty, station i	0.002 m
$\rho_{trop_{fluct}}$	Fluctuating troposphere uncertainty for 10 deg separation	0.01 m
$\rho_{iono_{day}_i}$	Daytime ionosphere model uncertainty (X-band level), station i	0.04 m
$\rho_{iono_{night}_i}$	Nighttime ionosphere model uncertainty (X-band level), station i	0.01 m

CCSDS REPORT CONCERNING DELTA-DOR—
TECHNICAL CHARACTERISTICS AND PERFORMANCE

Term	Description	Nominal Value
$\rho_{\text{iono}_{\text{fluct}}}$	Fluctuating ionosphere uncertainty for 10 deg separation (increase by $\times 2$ near solar max)	0.01 m
f_{RF}	Signal RF	8.42 GHz
B_s	Separation of raypaths from radio source to two stations, at plane of signal closest approach to Sun	6×10^6 m
V_{SW}	Solar wind velocity	4×10^5 m/s
ε_g	Quasar coordinate uncertainty	0.75×10^{-9} rad
B_p	Length of baseline projection onto plane-of-sky	8×10^6 m

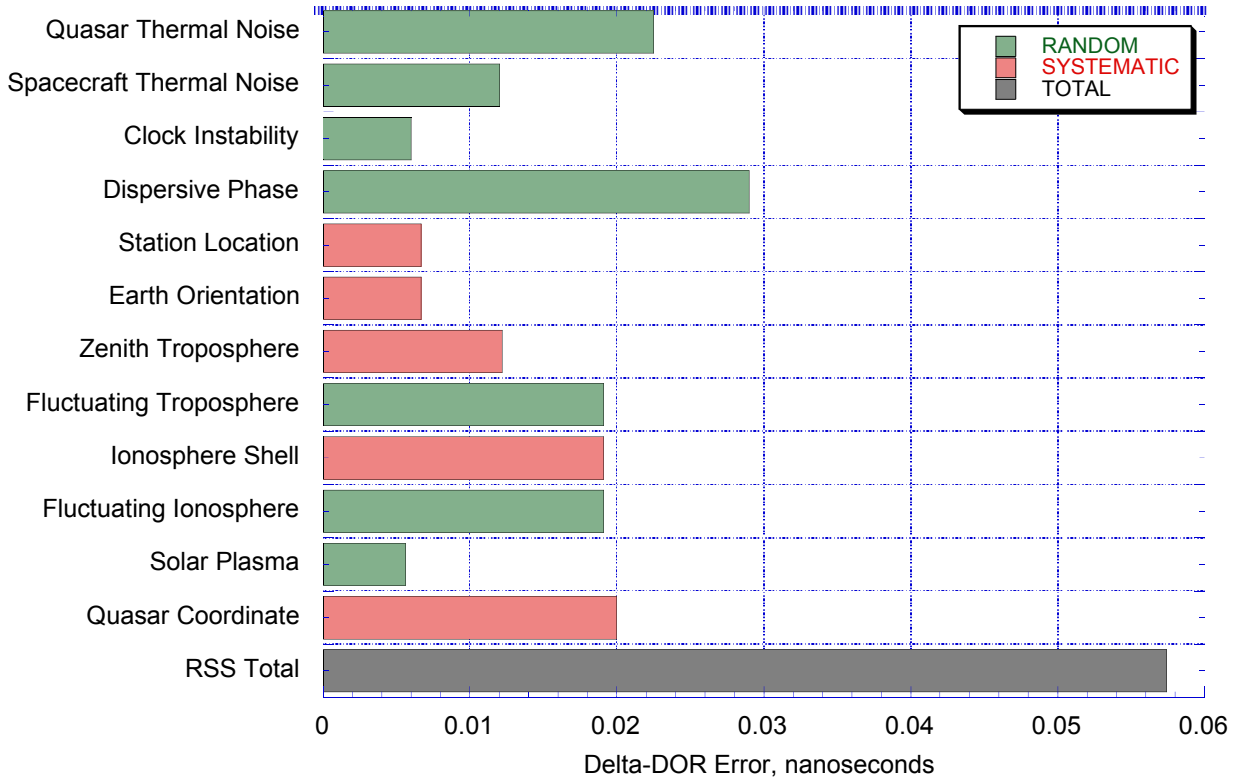


Figure 4-4: Delta-DOR Error Budget for X-Band Including Random and Systematic Effects (1 Sigma)

Table 4-2: Delta-DOR Error Budget (1 Sigma)—Both Random and Systematic Effects

<u>Component</u>	<u>Random/Systematic</u>	<u>Delay Error (ns)</u>
Quasar thermal noise	Random	0.023
Spacecraft thermal noise	Random	0.012
Clock instability	Random	0.006
Dispersive phase ³	Random	0.029
Station location	Systematic	0.007
Earth orientation	Systematic	0.007
Zenith troposphere	Systematic	0.012
Fluctuating troposphere	Random	0.019
Ionosphere shell	Systematic	0.019
Fluctuating ionosphere	Random	0.019
Solar plasma	Random	0.006
Quasar coordinate	Systematic	0.020
<hr/>		
RSS total		0.057

Table 4-3: Delta-DOR Error Budget (1 Sigma)—Random Effects Only

<u>Component</u>	<u>Delay Error (ns)</u>
Quasar thermal noise	0.023
Spacecraft thermal noise	0.012
Clock instability	0.006
Dispersive phase	0.029
Fluctuating troposphere	0.019
Fluctuating ionosphere	0.019
Solar plasma	0.006
<hr/>	
RSS random	0.048

³ Assuming sinusoidal DOR tone.

Table 4-4: Delta-DOR Error Budget (1 Sigma)—Systematic Effects Only

<u>Component</u>	<u>Model Error</u>
Station Location *	2 cm with correlations
Earth Orientation	
UT1 1-day prediction	2 cm
UT1 after the fact	1 cm
Polar Motion	1 cm
Zenith Troposphere	
Wet	0.5 cm
Dry	0.2 cm
Ionosphere Shell	
Day (X-band level)	4 cm
Night (X-band level)	1 cm
Quasar Coordinate	0.75 nrad

*Correlations among station coordinates may be accounted for in a covariance matrix.

5 SYSTEM RATIONALE AND TRADE-OFFS

5.1 DEFINITION OF PARAMETERS USED IN DELTA-DOR TRADE-OFFS

5.1.1 GENERAL

Delta-DOR measurements are affected by spacecraft-transmitter specifications, by ground-station-receiver specifications, and by the observing sequence and duration. This section discusses the design options that can be varied.

The measurements used for Delta-DOR are group delay measurements, and they require a signal that spans some bandwidth. Since weak extragalactic radio sources are observed for calibration, a spanned bandwidth of at least a few MHz is necessary. Group delay measurement performance generally depends on signal power and on the frequency span of the signal. Many different waveforms could be used, such as broadband noise (used for quasar measurements), pseudo-noise codes (used for spacecraft ranging), sinusoidal tones (also used for spacecraft ranging), or telemetry sidebands. In order to provide performance at a known level, and to enable interoperability, a standard has been recommended for spacecraft signal specification.

It is recommended that a spacecraft transponder emit several tones (referred to as DOR tones) spanning some bandwidth to enable a DOR measurement. CCSDS document 401.0-B (2.5.6B), listed as reference [5], describes the DOR tones, characterizes the spacecraft generation of the tones, and discusses how they may be detected/received at the ground stations. SFCG Recommendation 23-2 (reference [23]) and SFCG Recommendation 30-1 (reference [24]) also concern bandwidth and power considerations for the DOR tones.

Specifications for the spacecraft transponder and for ground station receivers must be consistent with the DOR tone Recommended Standards in order to enable inter-agency Delta-DOR measurements. It should be noted that DOR tones do not need to be at one exact frequency. Rather, a range of frequencies could be used to provide a Delta-DOR capability over a range of performance values. A general description of DOR tones is presented here, along with considerations that factor into design choices. The description given here helps explain the specification given in reference [5]. Equations in section 4 of this document support the general statements given here on performance trade-offs.

5.1.2 DOR TONE DESIGN CONSIDERATIONS

Mission navigation accuracy requirements and other spacecraft and planetary ephemeris accuracy requirements drive the considerations of this section.

Factors considered in design trade-offs for DOR tones include:

- a) Frequency band: The DOR tones may be at S-band (2290–2300 MHz), X-band (8400–8450 MHz), or Ka-band (31.8–32.3 GHz). Choice of downlink band is usually decided early in a mission design phase and depends on important factors

other than DOR tones. However, the choice made will impact Δ DOR performance. Charged particle effects in delay measurements scale as 1 divided by frequency squared, so the higher RF bands provide better accuracy when other factors are the same. Further, more spanned bandwidth has been allocated for deep space tracking at the higher RF bands, allowing the trade in b) to be considered. The higher bands allow for reducing certain error terms, since the DOR tone frequency may be selected up to the available spectrum allocation. But additional work may then be required to reduce other error terms in order to achieve an overall improvement in accuracy. For example, quasar flux tends to be lower at the higher frequency bands, and atmospheric attenuation tends to be higher, so channel sampling rate would need to be increased to maintain a high SNR. Further, fewer quasars are available for selection from existing catalogs, since surveying efforts at the higher frequency bands were started many years after similar efforts at the lower frequency bands. It should be noted that no need has yet been identified to extend this technique to Category A missions ('Near Earth') that operate in the K (25.5–27 GHz) band or Ka (37–38 GHz) band.

- b) Spanned bandwidth: The frequency separation between the two outermost DOR tones is referred to as the spanned bandwidth of the spacecraft signal. Generally, a narrow-spanned bandwidth is needed for integer cycle phase ambiguity resolution based on a priori knowledge of spacecraft angular position, while a wide-spanned bandwidth is needed for high measurement accuracy. (The same bandwidth span is used for both the spacecraft and the quasar to ensure instrumental error cancellation). The bandwidth span is a very important factor in terms of controlling errors due to spacecraft SNR, quasar SNR, and instrumental phase ripple, as these errors scale inversely with spanned bandwidth, so an overall improvement in performance is obtained by increasing the spanned bandwidth.
- c) Tone power to noise spectral density ratios: The SNR influences measurement accuracy. Also, there is a trade-off between SNR and the duration of the spacecraft scan. Higher SNR can be used either to achieve higher measurement accuracy or to reduce the overall measurement time needed to realize a specified accuracy.
- d) Waveform and modulation type: The DOR tones are generated by modulating a sine wave or square wave subcarrier onto the downlink carrier. The subcarrier waveform may itself either be modulated or unmodulated. An unmodulated subcarrier results in a spectrum of sinusoidal signals that are used for the Delta-DOR measurement. During a measurement session, receivers are configured to record frequency channels centered on the received DOR tones. The same frequency channels must be used for both the spacecraft and quasar in order for the quasar measurement to provide a calibration of instrumental delay for the spacecraft measurement. The frequency channels must be wide, on the order of 2-8 MHz, to detect the weak signals from natural radio sources. When the spacecraft signal is narrow bandwidth, the instrumental delay experienced by the spacecraft signal will not be identical to the instrumental delay experienced by the broadband quasar signal. The spacecraft sees the phase delay at one discrete frequency near the channel center while the quasar sees the average phase delay over the full channel bandwidth. This instrumental

delay difference is one of the dominant measurement errors for Delta-DOR. This error source could be reduced, or nearly eliminated, if the subcarrier were modulated by a Pseudo Noise (PN) code that effectively spreads the spacecraft signal power over the full channel bandwidth used for recording the quasar signal.⁴ In this case, instrumental effects on the two signal paths would be more nearly equal.

- e) Modulation parameters: Sine waves are normally used in multi-tone systems based on efficiency considerations. Modulation options include use of two sinusoidal waveforms phase modulated on the downlink carrier signal, one square wave phase modulated on the downlink carrier, and the user's choice of modulation indices. When multiple tones are provided, relatively more power is preferred in the outermost tones, since these are used to develop the final observable. Square wave harmonics drop off in amplitude as $1/n$, so they do not provide optimal performance. When multiple sine waves are used, a separate modulation index for each tone can be selected to place most power in the outer tones while providing just enough power to the inner tones to resolve the ambiguity.
- f) Number of DOR tones (1, 2, or 3): The number of DOR tones is largely determined by the band of the DOR tones. To provide higher performance (i.e., a wider spanned bandwidth with more power in the outer tones), while still providing a spanned bandwidth narrow enough for integer cycle ambiguity resolution, more DOR tones are needed. The minimum tone separation is based on the accuracy that can be guaranteed in the predicted ephemeris used during data processing. Once the ambiguity has been resolved for one bandwidth, it is generally possible then to resolve the ambiguity for a bandwidth that is wider by a factor of 20 to 80 (refer to 3.4).

NOTE – If a transponder also has the capability to generate a telemetry subcarrier, at a frequency comparable to the low frequency DOR tones, then it may be possible to use telemetry sidebands for ambiguity resolution, removing the need for low-frequency DOR tones.

- g) Tone frequencies: There is a trade-off between (i) choosing the widest possible bandwidth for improved measurement accuracy, (ii) placing the signal within the band allocated for deep space tracking, and (iii) keeping the spectrum compact to avoid interference from or to other users. Historically, 19 MHz has been used as the DOR tone frequency at X-band, and this sets a limit on the Delta-DOR measurement accuracy that can be achieved. The wider bandwidth allocation at Ka-band allows for the possibility of improved accuracy. For this reason, DOR tones at higher frequency are foreseen for Ka-band in reference [5]. To realize improved accuracy, even higher tones may be considered in the future. Surveys indicate that natural radio sources have correlated flux, over longer baselines, that is typically reduced by a factor of 2 to 3 from the X-band flux. There are sources with different spectral types and exceptions, but the typical behavior is relevant for support of navigation that requires a large catalog of quasars. Further, ground receivers have system noise temperatures

⁴ The use of a modulated subcarrier for generation of DOR signals is not presently covered in reference [5].

that are about a factor of 2 higher at Ka-band, when compared to X-band. The combination of these two effects implies, for the same DOR tone frequency, that the error due to system noise on the quasar measurement would be about five times higher at Ka-band as compared to X-band. Since this is typically one of the dominant Delta-DOR errors, overall Delta-DOR performance would degrade by this factor. To recover the same performance at Ka-band as for X-band, one could increase the DOR tone frequency by a factor of 4 and also increase the channel sample rate by a factor of 4. The combination of these two effects would reduce the system noise error on the quasar measurement by a factor of 8, providing slightly better performance at Ka-band than X-band. But to realize substantially better performance at Ka-band, it would be necessary to further increase the DOR tone frequency and/or channel sample rate.

- h) Coherency: The DOR tones may be a coherent submultiple of the downlink carrier, or they may be generated from an independent oscillator onboard the spacecraft. Either method provides comparable performance when DOR-tone SNR is high enough for standalone tracking, for example, 10 dB•Hz or greater. But, if the DOR tone is weaker than this, and if carrier aiding is used to detect the DOR tones, then performance is better if the DOR tone is coherent with the carrier. There is no advantage in having the downlink carrier coherent with an uplink signal as long as the one-way downlink carrier can itself be detected and tracked.
- i) Support for legacy missions: At present, both telemetry sidebands and uplink range codes have been used to enable Delta-DOR measurements on spacecraft without dedicated DOR tone modulation. While these signals may be used, they generally provide less spanned bandwidth than DOR tones and hence provide poorer performance. Delta-DOR measurement accuracy tends to scale linearly with inverse spanned bandwidth for bandwidths below 10 to 20 MHz.

5.1.3 GROUND STATION RECEIVER DESIGN CONSIDERATIONS

Factors considered in design trade-offs for ground station receivers and recorders include:

- a) Hardware compatibility: A standard set of nominal sample rates and sample quantization levels must be agreed to. However, each agency is free to develop its own hardware for receiving and recording the signals from spacecraft and quasars, provided data can be translated into a standard format. Reference [13] is the CCSDS Recommended Standard for raw Delta-DOR data exchange. To be compatible with this standard, each Agency must be able to provide data that have been recorded using an open loop technique in a set of separate discrete frequency channels. The number of channels and center frequencies to be used for the channels must be settable to a list of values that would vary for each spacecraft, and may also vary from one recording session to the next. The channel sample rate and sample quantization levels must be chosen from a list of agreed common values. Known current capabilities of CCSDS Member Agencies are given in section 6.

- b) Configuration flexibility: The specific tracking scenarios that will be supported (e.g., a single spacecraft in cruise or several spacecraft that are angularly close to each other) have implications for the number of frequency channels and the channel placements that are needed. Tracking passes that provide navigational support for several spacecraft are more efficient in terms of antenna resources, but put more demands on configuration of recording systems.
- c) Receiver parameters: Specification of the receiver performance characteristics (e.g., linearity of the phase-frequency response over each frequency channel, channel center frequency, sample rate, number of bits per sample, number of frequency channels) is required in order to plan observations and estimate overall system performance using the analysis of section 4. Several alternate levels of instrumental performance (e.g., different sample rates and different frequency spans) could be specified that would correspond to different levels of Delta-DOR accuracy.
- d) Instrumental delay stability: The instrumental delay must be kept the same over the duration of the measurement session, and the same for both spacecraft and quasar, within the limits imposed by variations in analog components. If different channel sampling rates are used for the spacecraft and the quasar, then the filter delay should be compensated so that both spacecraft and quasar will experience the same signal delay. If an antenna array is used to receive the signal, the position and clock reference point for the array must remain fixed.

5.1.4 RADIO SOURCE SELECTION AND OBSERVATION SEQUENCE CONSIDERATIONS

Factors considered for radio source selection and observation setup include:

- a) Source selection: Ideally, one would observe a strong, compact radio source that is angularly close to the spacecraft trajectory. As a starting point, the X-band radio source catalog (reference [6]) is usually dense enough to provide a single source, or two sources with an ‘effective average position’, that falls within 6 deg of a given spacecraft angular location and has flux density of 0.4 Jy or above. The options are to select a stronger source that is more angularly distant or to select a weaker source that is angularly closer. Some error sources scale up as flux decreases while other error sources scale down as angular separation decreases. Source selection thus has a large impact on overall performance. More options in recording system sensitivity (G/T , sample rate, spanned bandwidth) provide more options for source selection. Also, continuing survey work to add sources to the catalog provides more options for source selection. But it should be recognized that there are not many sources (discovered or undiscovered) that have flux exceeding 0.4 Jy. Limits imposed by the spanned bandwidth of current spacecraft and by the sensitivity of current ground stations make it impractical to select sources with flux much below 0.4 Jy, so options are limited at present.

NOTE – Source flux is variable, and survey measurements of source flux should be repeated over time.

- b) Observation sequence: The length of each scan, the number of alternate spacecraft and quasar observations, and the total duration of the measurement session can be adjusted. Times are usually kept short to reduce station usage and to complete observations at higher station elevation angles. Since SNR improves only as the square root of observation time, and long baselines have limited viewing overlaps, not too much can be gained by increasing observation time. On the other hand, the observation time needs to be at least a few minutes per source, or else short period media fluctuations will begin to dominate, and thermal noise errors will grow. As a starting point, 5–10 minutes per scan and six alternate spacecraft and quasar observations should be considered. This strategy controls temporal media fluctuations to the level stated in section 4 of this document and allows for internal validation of the data.
- c) Channel sample rate: A higher sample rate increases quasar SNR, but the channel bandwidth cannot be more than $\frac{1}{2}$ the spanned bandwidth if quasar channels are to be independent and aligned with spacecraft channels. Generally, it is necessary to keep the quasar channel bandwidth down to the level of about $\frac{1}{10}$ the spanned bandwidth in order for the phase ripple error to not exceed the value given in table 4-1. Using a wider channel bandwidth for the quasar would be expected to result in poorer cancellation of dispersive phase error between spacecraft and quasar.

NOTE – This limitation might be avoided if the spacecraft were to transmit a spread-spectrum–like quasar noise rather than pure tones, or if the non-linear phase response of the receiver bandwidth could be well calibrated.

5.2 TRADE-OFF ON SPACECRAFT TONE POWER

The Delta-DOR error budget presented in 4.3 assumes a high spacecraft DOR tone SNR. This allows flexibility in meeting an accuracy requirement and more options for achieving higher performance. Alternatively, measurements could be made at lower tone powers but with reduced performance. The impact on spacecraft delay measurement precision and total delay accuracy can be calculated using the models of 4.3. Tables 5-1, 5-2, and 5-3 show the calculated value for the spacecraft thermal noise contribution ($\epsilon_{\tau_{SC}}$) and for the RSS total delay error ($\epsilon_{\Delta\tau_{RSS}}$) for a range of assumptions about the spacecraft tone SNR (P_{DOR}/N_0), the spacecraft observation time (T_{SC}), and the spanned bandwidth (f_{BW}). All other assumptions are kept at the nominal values, as given in table 4-1, that are based on typical NASA system performance.

In general, visibility is limited for long baseline measurements, so observation times will be limited. The total duration for a session is usually kept to 1 hour, and the duration of an individual scan is usually kept between 5 and 10 minutes. Table 5-1 presents results for the preferred case in which spacecraft observation time is set to 8 minutes, and the spanned

CCSDS REPORT CONCERNING DELTA-DOR—
TECHNICAL CHARACTERISTICS AND PERFORMANCE

bandwidth is close to 40 MHz. The measurements with low P_{DOR}/N_0 (first three rows) are dominated by thermal noise on the spacecraft measurement. Overall system performance improves significantly as P_{DOR}/N_0 is increased. The higher values of P_{DOR}/N_0 provide a more robust implementation in which overall system performance does not mostly depend on a single term, and more efficient use can be made of other system resources.

Table 5-1: Dependence of Delay Precision and Accuracy on Spacecraft Signal Parameters: High Performance Case

P_{DOR}/N_0 (dB·Hz)	T_{SC} (s)	f_{BW} (Hz)	$\epsilon_{\tau_{\text{SC}}}$ (ns)	$\epsilon_{\Delta\tau_{\text{RSS}}}$ (ns)
1	480	38.25×10^6	0.239	0.246
7	480	38.25×10^6	0.120	0.133
13	480	38.25×10^6	0.060	0.082
19	480	38.25×10^6	0.030	0.064
27	480	38.25×10^6	0.012	0.057

Table 5-2 presents results for a case in which spacecraft tone power may be limited, due perhaps to transmission from a low gain antenna. Observation time is set to 30 minutes to partially compensate for reduced tone power. The spanned bandwidth is fixed at close to 40 MHz. The measurements with low P_{DOR}/N_0 are dominated by thermal noise on the spacecraft measurement, as before. But in this case, overall system performance improves little as P_{DOR}/N_0 is increased beyond the third row. The use of the longer scan duration shown in table 5-2 would be appropriate only for the lower tone powers of rows 1–3. This represents the use of the Delta-DOR system to meet a mission need in which spacecraft tone power is constrained despite ground station resources being used in an inefficient manner.

NOTE – Visibility conditions do not always allow for such a long scan time.

Table 5-2: Dependence of Delay Precision and Accuracy on Spacecraft Signal Parameters: Low Gain Antenna Case

P_{DOR}/N_0 (dB·Hz)	T_{SC} (s)	f_{BW} (Hz)	$\epsilon_{\tau_{\text{SC}}}$ (ns)	$\epsilon_{\Delta\tau_{\text{RSS}}}$ (ns)
1	1800	38.25×10^6	0.124	0.136
7	1800	38.25×10^6	0.062	0.084
13	1800	38.25×10^6	0.031	0.064
19	1800	38.25×10^6	0.016	0.058
27	1800	38.25×10^6	0.006	0.057

Table 5-3 presents results for a case in which the spacecraft does not have DOR tones or else only has a low-frequency DOR tone. Observation time is set to 30 minutes, and the spanned bandwidth is fixed at 6 MHz. Some legacy missions have been supported using parameters with values similar to the values shown in table 5-3. While overall performance does not compare to what can be achieved using the assumptions in table 5-1 or table 5-2, the resulting performance may be of benefit to some mission classes.

Table 5-3: Dependence of Delay Precision and Accuracy on Spacecraft Signal Parameters: No DOR Tone or Low Frequency DOR Tone Case

P_{DOR}/N_0 (dB•Hz)	T_{SC} (s)	f_{BW} (Hz)	$\epsilon_{\tau_{\text{SC}}}$ (ns)	$\epsilon_{\Delta\tau_{\text{RSS}}}$ (ns)
1	1800	6×10^6	0.788	0.823
7	1800	6×10^6	0.395	0.461
13	1800	6×10^6	0.198	0.310
19	1800	6×10^6	0.099	0.258
27	1800	6×10^6	0.040	0.241

The nominal values for the observation assumptions of 4.3 are shown in table 5-1 in the 5th row, highlighted in bold. This row satisfies the good engineering practice of having each error source that can be controlled kept at no more than 25 percent of the total error budget. It should be noted that most rows with lower SNR assumptions do not satisfy this criterion.

5.3 THE ACHIEVABLE PERFORMANCE – X-BAND

Based on the above discussion in 5.1.1 to 5.1.3, and the error sensitivity equations in section 4, the most important parameters for Delta-DOR observation trade-off on X-band performance are those listed in table 5-4. The nominal values for the parameters in table 5-4 are consistent with table 4-1.

Table 5-4: Nominal Parameter Values for Evaluation of Δ DOR Trade-Offs at X-Band

Term	Description	Nominal Value
$\Delta\theta$	Angular separation between SC and QU	0.1 rad
D	Channel sampling rate	16×10^6 samples/s
f_{BW}	Spanned bandwidth	38.25×10^6 Hz
<i>Band</i>	RF band	X-band
S_c	Quasar correlated flux	0.4 Jy
ϵ_g	Quasar coordinate uncertainty	0.75×10^{-9} rad
	DOR signal structure	Sinusoidal
	Dispersive Phase error reduction with PN DOR	$\times 10$

The parameters and nominal values in table 4-1 define a typical Delta-DOR observation, and are the starting point for trade-off considerations. This subsection looks at variations in the specific parameters listed in table 5-4. These trades are based on current system capabilities.

Surveys have been made of the density of quasars per unit area on the celestial sphere at a given flux level. Generally, it is necessary to select a quasar with smaller S_c in order to obtain a smaller $\Delta\theta$. It was stated in 5.1.3 that there is usually a quasar with flux 0.4 Jy within 6 deg of a spacecraft to be observed. For this trade-off study, it is assumed that the available quasar flux will change linearly as $\Delta\theta$ (rad):

$$S_c = \frac{0.4}{0.1} \Delta\theta \text{ Jy.} \quad (33)$$

Based on surveys (references [14], [15], and [16]), this assumption is plausible over the range of 1–15 deg separation angles typically used for an X-band Delta-DOR observation. But it is noted in reference [14] that these survey results are preliminary and research continues in this area.

Using the assumption represented by equation (33), the RSS total Delta-DOR error for X-band observations may be plotted as a function of $\Delta\theta$. This is shown in figure 5-1 for both sinusoidal and PN DOR at $f_{\text{BW}} = 38.25$ MHz, and for sinusoidal DOR at $f_{\text{BW}} = 76.5$ MHz. The wider spanned bandwidth is possible in some cases by using the second harmonic of the DOR tone. The curve showing estimated total error has a shallow minimum at a separation angle of 0.09 rad for the nominal spanned bandwidth of 38.25 MHz sinusoidal. As separation angle grows, errors that scale with separation angle dominate, and the RSS total error is nearly a linear function of $\Delta\theta$. As $\Delta\theta$ gets small, the error due to quasar thermal noise grows fast and completely dominates, since it is assumed that a correspondingly weak quasar must be observed. If the spanned bandwidth could be increased, then the minimum error would be reduced, and the minimum would occur at a smaller value of $\Delta\theta$. The curve for a factor of two increase in f_{BW} is shown. A larger increase in f_{BW} is not considered practical since allocated bandwidth in the 8.4 GHz space research band is limited.

The curve for PN DOR at $f_{\text{BW}} = 38.25$ MHz lies between the two curves for sinusoidal modulation. The improvement in switching from sinusoidal to PN DOR appears modest, but one should keep in mind that conservative assumptions have been used in the error budget. The assumptions used in the error budget are intended to provide an estimate of accuracy that users can count on for tracking anywhere in the ecliptic region. Under more favorable geometry, such as a small angular separation from a strong quasar, the phase dispersion term is the only large term in the error budget. This term is reduced by a factor of ten with PN DOR.

Still, the achievable performance at X-band is limited. The minimum error shown in figure 5-1 is only a factor of two larger than the quasar coordinate uncertainty.

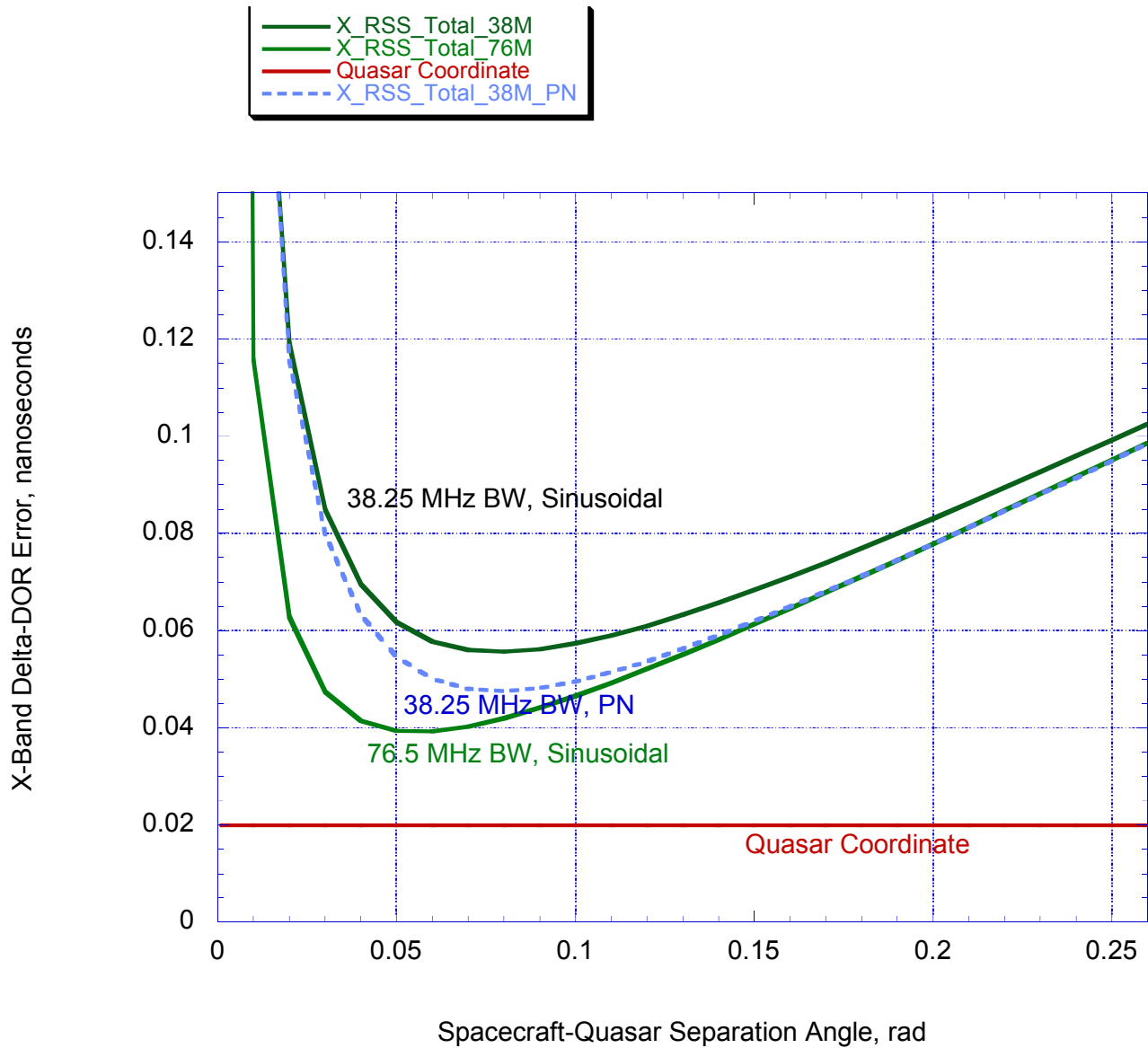


Figure 5-1: Estimated Delta-DOR Performance, 1 Sigma, at X-Band As a Function of Spacecraft-Quasar Separation Angle

5.4 THE ACHIEVABLE PERFORMANCE – KA-BAND

There are several factors that limit Δ DOR performance at X-band and make it difficult to build a system that would generally perform much better than the curves shown in figure 5-1. Of course, there are special situations, such as for a spacecraft angularly close to a strong quasar, that would have better performance. But in general, X-band performance is limited by

- X-1: restricted bandwidth in the 8.4 GHz space research band;
- X-2: tropospheric and ionospheric fluctuations; and

- X-3: coordinate uncertainty and structure effects in quasar core locations.

NOTE – It has been suggested that performance could be improved for X-band Delta-DOR by observing a very strong quasar to calibrate the phase response of the passband over a wider frequency span. Then, for the reference source, a weaker quasar that is angularly closer to the spacecraft is selected. While the spacecraft can only be observed over its transmitted frequency span, this quasar can be observed over the wider and now calibrated frequency span. The utility of this approach would depend on the smoothness of the phase response of the passband to be calibrated, the temporal stability of the phase response, and the availability of very strong calibrator sources. No experimental results are available to report on at this time.

Delta-DOR performance could be improved by using spacecraft downlinks at Ka-band instead of X-band. The potential improvements, corresponding to the X-band limitations just stated, include:

- Ka-1: wider bandwidth allocation in the 32 GHz space research band would enable increased spanned bandwidth and higher quasar channel sampling rates;
- Ka-2: charged particle effects are reduced by the square of the frequency ratio;
- Ka-3: radio sources tend to be more compact at the higher frequencies so that core locations could be determined with higher accuracy.

Ka-band also has drawbacks, which tend to reduce performance. Some of these may be overcome, and final performance will depend on related developments. Six significant differences between X-band and Ka-band, affecting accuracy, are discussed in items a) through f), below. The expected factor difference between X-band and Ka-band is stated.

- a) Quasar flux is reduced by a factor of 2.5.

Radio sources emit flux that follows power law distributions. On average, flux S_ν from the compact core of extragalactic radio sources depends on observing frequency ν according to $S_\nu \propto \nu^{-0.65}$ (reference [14]). This corresponds to a reduction in flux of approximately a factor of 2.5 for Ka-band relative to X-band.

- b) System noise temperature is increased by a factor of 2.

Atmospheric attenuation and noise temperature are related and depend on the observing frequency (references [17] and [18]). There can also be significant variations due to site location, elevation angle, and weather conditions. Curves of mean effective (i.e., including effects due to antenna microwave, atmospheric attenuation, and atmospheric noise) system temperature have been generated for NASA Deep Space Network (DSN) sites for a range of assumptions (reference [18]).

For example, system temperature is 27 K at X-band for DSN 34m antenna 26 at Goldstone, assuming 0.5 cumulative distribution weather and 20 deg elevation angle

(reference [18], figure 26), while system temperature is 54 K at Ka-band for these same assumptions (reference [18], figure 36).

Differences are larger for poorer weather conditions and for lower elevation angles. Here it is assumed effective system temperature is a factor of 2 higher at Ka-band than at X-band.

- c) Quasar channel sampling rate is increased by a factor of 4.

The capability exists today to record at a much higher rate than was assumed in table 4-1 for X-band. But any increase in sampling rate must be tempered by the trade-off discussed in 5.1.3c) that wider channels have a less linear phase response than narrow channels. The assumption here is to increase the sampling rate by just the same amount as the spanned bandwidth (see d)).

- d) Spanned bandwidth is increased by a factor of 4.

The spectrum allocation for space research is 10 times wider at Ka-band than for X-band, so conceivably, the spanned bandwidth could be increased by a factor of 10. However, spacecraft electronic components may not support the full available bandwidth. Here is made a conservative assumption that DOR tone frequency for Ka-band will be four times that currently in use at X-band. This assumption is also consistent with reference [5].

- e) Charged particle effects are reduced by a factor of 15.

It is known that signal delay caused by passage through charged particles scales inversely as frequency squared. The effect of the ionosphere and solar plasma will be reduced by a factor of 15.

- f) Quasar coordinate error is reduced by a factor of 3.

The cores of extragalactic radio sources tend to be more compact and more stable at higher frequencies (references [20] and [21]). It follows that, given sufficient multi-baseline VLBI observing sessions, it will be possible to build a more accurate radio source catalog at Ka-band. There is little doubt that quasar coordinates could be determined to the level of 0.25 nrad if enough effort is devoted to this task. Here it is assumed a factor of 3 improvement in coordinate accuracy relative to the (conservative) estimate given in table 4-1 for X-band.

The six items above are straightforward effects of the transition from X-band to Ka-band. Figure 5-2 shows estimated Δ DOR performance at Ka-band. All assumptions are the same as in table 4-1 except for the factors identified in items a) through f), above. As in figure 5-1, curves are shown for the RSS total error as a function of separation angle, for two different values of spanned bandwidth. The quasar coordinate error is also shown. Expected performance at Ka-band is about a factor of 2 better than for X-band. Further, the performance shown here for Ka-band is not yet at a fundamental limit. Additional advances could be made by:

- Ka-4: using PN DOR rather than sinusoidal DOR tones, to reduce Phase Dispersion error by a factor of 10;

CCSDS REPORT CONCERNING DELTA-DOR—
TECHNICAL CHARACTERISTICS AND PERFORMANCE

- Ka-5: better tropospheric calibration using an Advanced Water Vapor Radiometer (AWVR) and/or improved Global Navigation Satellite System (GNSS) observations, to reduce tropospheric errors by a factor of 2.

With these two advances, Δ DOR performance at Ka-band is improved by nearly another factor of 2, shown in figure 5-2 as a dashed curve. Table 5-5 shows the Ka-band error budget assumptions with respect to the X-band error budget assumptions shown in table 5-4.

Table 5-5: Nominal Parameter Values for Evaluation of Δ DOR Trade-Offs at Ka-Band

Term	Description	Nominal Value
$\Delta\theta$	Angular separation between SC and QU	0.1 rad
D	Channel sampling rate increase wrt X-band	$\times 4$
f_{BW}	Spanned bandwidth increase wrt X-band	$\times 4$
<i>Band</i>	RF band	Ka-band
ρ_{iono}	All ionospheric values given in table 4-1 reduced with Ka-band frequency	$\times 14.5$
S_c	Quasar correlated flux decrease wrt X-band	$\times 2.5$
ε_g	Quasar coordinate uncertainty	0.25×10^{-9} rad
G	Antenna Gain	$\times 14.5$ [+11.6 dB]
T	System noise temperature	$\times 2$ [−3dB]
ε_ϕ	Dispersive Phase error reduction with PN DOR	$\times 10$
ρ_{tropo}	All tropospheric values given in table 4-1 reduced with in-line WVR	$\times 2$

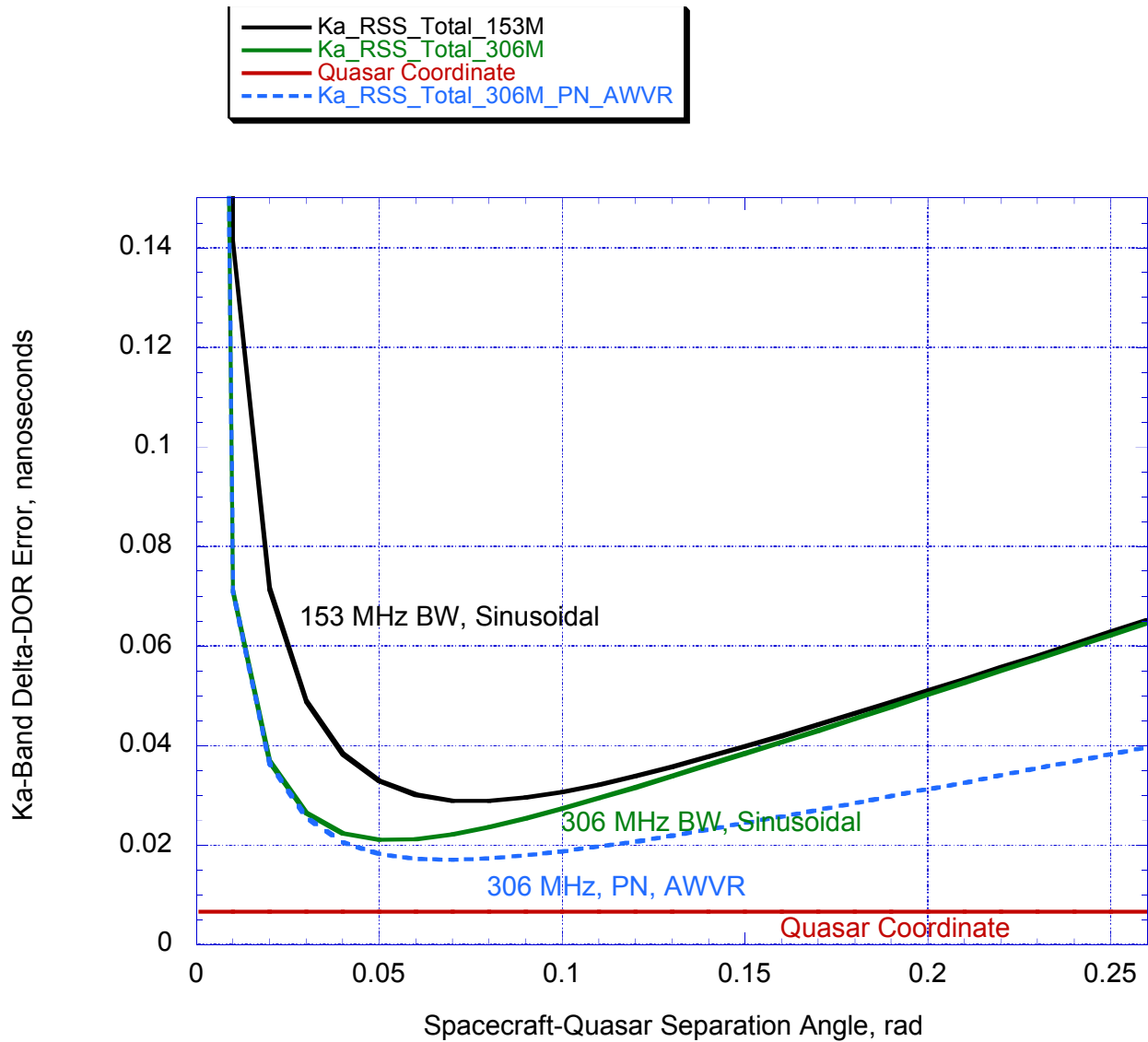


Figure 5-2: Estimated Delta-DOR Performance, 1 Sigma, at Ka-Band As a Function of Spacecraft-Quasar Separation Angle

It should be noted that the results given in figure 5-1 and figure 5-2 depend heavily on the assumptions that have been made. Assumptions have been based on current capabilities and on current understanding of the technique. Results could be quite different if, for example, more sensitive antennas were used, a higher data sampling rate were used, or quasar densities were more favorable than preliminary survey results suggest.

Also, the use of PN DOR allows more flexibility to obtain performance at various levels. With PN DOR, the channel bandwidth can be increased, reducing the error due to quasar thermal noise, while the spanned bandwidth and the error due to phase dispersion are not increased.

6 DESCRIPTION OF EXISTING SYSTEMS

6.1 THE NASA SYSTEM

6.1.1 GENERAL

The system to acquire Delta-DOR data at a NASA DSN station consists of the antenna, the microwave components, frequency and timing signals, and the open loop receiver used for VLBI data recording. DSN stations have two separate VLBI recorders: the Mark V system used primarily for radio astronomy and the Open Loop Receiver (OLR) (reference [12])⁵ used primarily to support Radio Science and Delta-DOR. Only the OLR is described in this section.

6.1.2 FUNCTIONAL SPECIFICATIONS

A simplified block diagram of the end-to-end Delta-DOR system is shown in figure 6-1. RF signals received at an antenna are input to a Low Noise Amplifier (LNA). A mixer driven by a fixed Local Oscillator (LO) is used to downconvert the signal from RF to an Intermediate Frequency (IF) of about 300 MHz. The analog IF signal is fed to the IF Gain Control (IGC) assembly, where the signal level is adjusted to the proper level for digitization. Normally, analog gain is adjusted just once at the beginning of each tracking pass. The signal is then fed to an IF Digitizer (IFD) that breaks the input bandwidth of 525 MHz into digital packets of bandwidth 6.25 MHz each. All packets are sent to a 10 Gb Digital IF Switch (DIS) that broadcasts the desired groups to the OLR upon request.

The DIS receives signals from each available antenna, RF, and polarization. The switch allows each OLR to select from any of the IF signals feeding the DIS. Each output of the DIS feeds digital packets into one input of the OLR Real-time Signal Processor (RSP). The Advanced Mezzanine Card (AMC) in the RSP synthesizes the requested channel bandwidths and provides baseband channels to the Data Processing and Control (DPC) computer for recording on the RAID storage.

The OLR has 16 independent frequency channels. Each channel is from 1 kHz to 100 MHz wide. The channel center frequency can be at any place in the IF bandpass with a resolution of 1 Hz. The channel center frequency may either be fixed or tuned to follow the spacecraft Doppler predict. The channels may be reconfigured between scans. Typically, a wider channel bandwidth is used for quasar signal recording, while a narrower channel bandwidth is used for spacecraft signal recording. The filter delays for each channel are compensated so that each channel, regardless of bandwidth, has the same digital signal delay. The LOs for all channels are phase coherent.

Functional specifications for the Delta-DOR system are given in table 6-1.

⁵ This reference currently describes the predecessor to the OLR, which is the Wideband VLBI Science Receiver (WVSR). The reference will be updated to describe the OLR.

Table 6-1: Functional Specifications for the NASA Delta-DOR System

Parameter	Value	Remarks
ANTENNA		
Polarization	RCP and LCP	
LNA		
Frequency ranges covered		
S-band	2200–2300 MHz	
X-band	8200–8600 MHz	
Ka-band	31800–32300 MHz	
First LO		
S-band	2000 MHz	
X-band	8100 MHz	
Ka-band	31700 MHz	
OLR		
Digital IF input range	10-610 MHz	
Minimum time between recording intervals (scans)	16 seconds	To allow for antenna slew and change configuration
Independent Channels		
Number of Channels	16	
Narrow bandwidths	Many bandwidths, including 1, 2, 4, 8, 16, 25, 50, 100, 200, and 500 kHz	
Wide bandwidths	Many bandwidths, including 1, 2, 4, 8, 16, 32, 50, and 100 MHz	
Sample Resolution	1, 2, 4, 8, or 16 bits/sample	
Digital downconversion	Sub-Hz resolution	Fixed frequency or tuned to Doppler predicts
Sample format	In-phase and Quadrature-phase (I/Q)	
Maximum allowed recording rate	512 Mbits/s	Number of channels, bandwidth, and resolution must be chosen to not violate this constraint

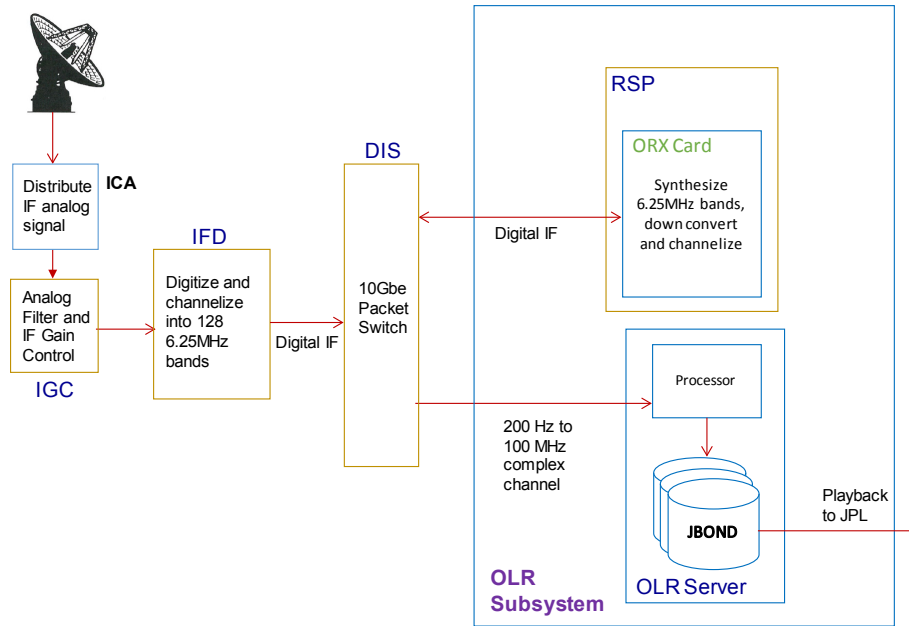


Figure 6-1: Simplified Block Diagram of Delta-DOR System in the NASA Deep Space Network

6.1.3 OPERATIONAL INTERFACES

Flight projects and other external users acquire services from the DSN by first negotiating a tracking schedule. The schedule identifies the spacecraft to be tracked, the tracking stations to be used, the time interval for the track, and whether the track includes a Delta-DOR measurement. For each scheduled Delta-DOR track, the user must provide sequence information to the DSN in the internal format required by the DSN. The sequence inputs are essentially the station configuration to be used, the RF band(s) of the downlink signal, and the sequence of events to be executed. The DSN then internally generates support products necessary to control the station and provide the service.

For Delta-DOR, a set of configuration files is maintained on the OLR to specify the setup of the frequency channels to be recorded. There is typically one such configuration file for each spacecraft, but multiple configurations could be defined to support, for example, recordings at different sample rates or recordings of different spectral components. These configuration files are based on the spacecraft signal characteristics and normally do not change over the lifetime of a mission. For each scheduled pass, the DSN generates two types of support products from the user-supplied sequence information and from other required data supplied by the user, including spacecraft ephemeris and transmitter frequency. The two support products are

- a) antenna predicts to control the slewing between spacecraft and quasars; and
- b) OLR predicts that identify the configuration file to be used, include a table of spacecraft and radio source recording intervals (scans), and include predicts for the received center frequency of the spacecraft downlink.

These two predict sets are derived from the same project inputs and hence will be consistent with each other, but during a tracking pass, the antenna and the OLR are operated independently.

When OLR predicts are received, the OLR generates a script based on the predicts and on the named configuration file. This script then controls the operation of the OLR during the pass. Data files in the native format of the OLR are stored locally on the OLR disks. Data files for a scan are available for playback (i.e., transfer over a network interface) as soon as that scan has been completed. Data transfer is initiated by a request from a server at a correlator facility.

When playback of the data for a scan has been completed from two stations, correlation processing may begin. Quasar data are cross-correlated and a fringe-fitting program is run to extract the cross-correlation phase for each frequency channel. For spacecraft data, the phase is measured for each tone at each of the stations. When data for all scans have been processed through this stage, time delay observables for the full pass are then generated, validated, and made available to the navigation customer.

6.2 THE ESA SYSTEM

6.2.1 GENERAL

The system to acquire Delta-DOR data at an ESA Deep Space Antenna consists of the antenna front-end, the microwave components (LNA and a DownConversion (DC) stage), and finally, the open loop functionality of the Tracking, Telemetry, and Command Processor (TTCP). DC and TTCP are driven by Frequency and Timing signals.

6.2.2 FUNCTIONAL SPECIFICATIONS

A simplified block diagram of the back-end part of the system is shown in figure 6-2. Before reaching the DC stage, RF signals received at the antenna are input to an LNA. After the amplification stage, they are downconverted to the IF band. The signal at IF then reaches the TTCP, where it is digitized. Up to 16 independent frequency subchannels can be simultaneously recorded in open loop by the TTCP, after digital downconversion and filtering of the IF input. The bandwidth of these subchannels can be set from 1 kHz to 16 MHz (in exact 1 kHz steps and with different bits resolution), while the center frequency can be configured with better than 1 Hz resolution. The subchannel center frequency may either be fixed or tuned to follow the spacecraft Doppler predictions. The data for each frequency channel are then formatted in Delta-DOR Raw Data Exchange Format (RDEF) and recorded into an internal TTCP disk.

The channels may be reconfigured between scans. Typically, a wider channel bandwidth is used for quasar signal recording while a narrower channel bandwidth is used for spacecraft signal recording.

CCSDS REPORT CONCERNING DELTA-DOR—
TECHNICAL CHARACTERISTICS AND PERFORMANCE

Functional specifications for the Delta-DOR system are given in table 6-2.

Table 6-2: Functional Specifications for the ESA Delta-DOR System

Parameter	Value	Remarks
ANTENNA		
Polarization	RCP and LCP	
LNA		
Frequency ranges covered		
S-band	2200–2300 MHz	New Norcia only
X-band	8400–8500 MHz	
Ka-band	31800–32300 MHz (in 220 MHz chunks)	Not available at New Norcia (as of 2019). New converter planned, with 500 MHz BW.
DC		
S-band LO	2720 MHz	New Norcia only
X-band LO	9040 MHz	
Ka-band: 1 st LO Ka-band: 2 nd LO	22400 MHz Variable (8780–9480 MHz)	Not available at New Norcia (as of 2019). 1.55 GHz IF on future converter.
TTCP		
Analog IF input range	Medium Band: 220 MHz Wide Band: 600 MHz	
Minimum time between recording intervals (scans)	90 seconds	To allow for antenna slew and change configuration
Subchannels (i.e., recordable channels)		
Number of subchannels	16	
Narrow bandwidths with 8- or 16-bit resolution (bits/sample)	Any from 1 kHz to 100 kHz	
Wide bandwidths with 1, 2- or 4-bit resolution	16 MHz for 1 bit, 8 MHz for 2 bit, 4 MHz for 4 bit.	
Digital downconversion	Sub-Hz resolution	Fixed frequency or tuned to Doppler predicts
Sample format	In-phase and Quadrature-phase (I/Q)	
Maximum allowed record rate	512 Mbits/s	Maximum subchannel capacity is 32 Mb/s. Subchannel bandwidth and resolution must be chosen not to violate this constraint.

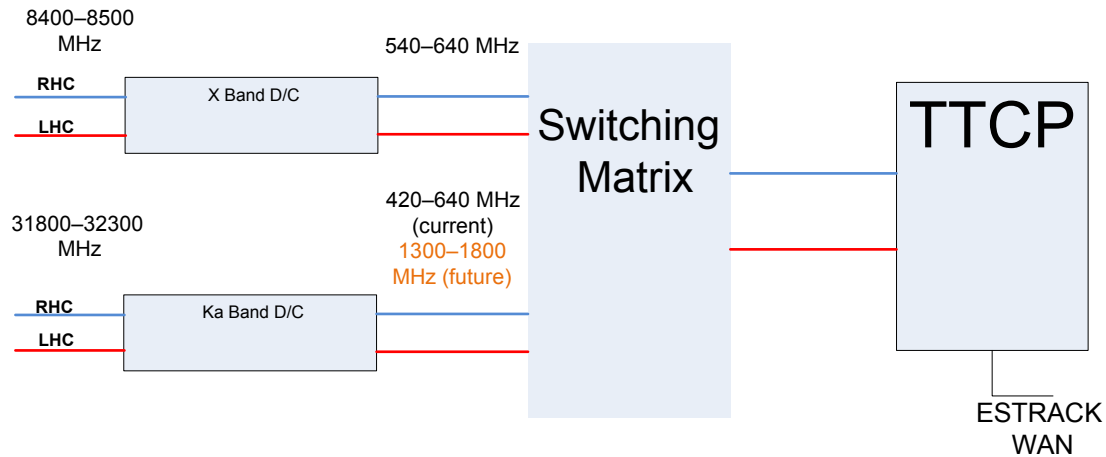


Figure 6-2: Simplified Block Diagram of Delta-DOR System in the ESA Deep Space Network (New Norcia S-Band Not Shown)

6.2.3 OPERATIONAL INTERFACES

Delta-DOR operational interfaces currently in use at ESA are briefly summarized here.

Normally, long-term schedules addressing all telemetry, tracking, and command services are created every six months. These high-level schedules identify the spacecraft to be tracked, the tracking stations to be used, and the time interval for the track. Then, for each scheduled Delta-DOR track, the user must provide detailed ‘sequence information’ to the ESA scheduling office in the internal format. The sequence inputs are essentially the station configuration to be used, the quasar(s) to be tracked, and the sequence of scans to be executed. ESOC scheduling office then internally generates the final schedule needed to control the station and provide the service. This schedule is transferred to the Station Computer at each station, which is in charge of handling the station configuration and operations derived from the user-supplied schedule.

For Delta-DOR, a set of configuration files is maintained on the TTCP to specify the setup of the frequency channels to be recorded. The configuration files are based on the spacecraft signal characteristics and normally do not change over the lifetime of a mission.

For each scheduled pass, the Flight Dynamics group at ESOC generates a spacecraft trajectory data message file, which is transferred to the station to generate further support products for the pass. The generation of such support products (i.e., pointing predicts and the TTCP configuration to be used) is automatically handled by the Station Computer,

Data files in RDEF format are stored locally at the antenna on a TTCP disk. Data files for a scan are available for playback (i.e., transfer over a network interface) as soon as that scan has been completed. Data transfer to the correlator facility (i.e., ESOC) is automated.

When playback of the data for a scan has been completed from two stations, correlation processing will be started and controlled by an operator. When data for all scans have been

processed, time delay observables for the full pass are generated, validated, and made available to the navigation customer. Some additional information (e.g., log files, plots, intermediate products of the correlation process) are kept for internal use and characterization of obtained results.

6.3 THE JAXA SYSTEM

6.3.1 GENERAL

The system to acquire Delta-DOR data at JAXA Deep Space stations consists of the antenna front-end, the microwave components all driven by frequency and timing signals generated from hydrogen masers, and the open loop receivers for VLBI data recording. The VLBI receiver used at JAXA stations is the K5 system, which conforms to the VLBI Standard Hardware Interface (VSI-H) established by the International VLBI Service for Geodesy and Astrometry (IVS) (reference [22]). Also, the raw data stream recorded through VSI-H interfaces can be duplicated and distributed directly to the local 10 GbE network.

6.3.2 FUNCTIONAL SPECIFICATIONS

A simplified block diagram of the back-end part of the system is shown in figure 6-3. The maximum number of four IF analog signals are distributed to a K5 receiver, and each IF signal is digitized, downconverted, and sent to the storage server via four VSI-H ports or two 10 GbE ports of the receiver. Unlike the NASA or ESA system, minimum output bandwidth is limited to 4 MHz. Further downconversion processing, required for narrowband spacecraft channels or quasar channels narrower than 4 MHz, is done in post processing with the back-end storage servers. Other post processing, such as spectrum analysis, gain control, and adding the RDEF header sections to the data stream, are performed in the storage server. The output data is saved as an RDEF file to the internal RAID6 array and is formatted with ext4 or xfs filesystem. The receiver has two independent output modes: digital downconversion mode and wide bandwidth output mode. Digital downconversion mode is used for nominal Delta-DOR passes, and wide bandwidth mode may be used for the purpose of calibrating wideband phase variation across the whole IF bands or for the observations with international radio telescopes outside the Delta-DOR network. The channels or recording modes may be reconfigured between scans. Typically, a wider channel bandwidth is used for quasar signal recording, while a narrower channel bandwidth is used for spacecraft signal recording. The filter delays and output time tag for each channel are compensated so that each channel, regardless of bandwidth, has no digital signal delay.

Functional specifications for the Delta-DOR system are given in table 6-3.

Table 6-3: Functional Specifications for the JAXA Delta-DOR System (Usuda Station)

LNA and analog receivers		
Frequency ranges covered		
L-band	1300–1750 MHz	RCP and LCP
S-band	2200–2350 MHz	RCP and LCP
C-band	4700–6700 MHz	RCP and LCP
X-band	8180–8680 MHz	RCP and LCP
First LO		
L-band	1200 MHz or 1250 MHz	
S-band	2020 MHz	
C-band	4600 MHz or 6400 MHz	
X-band	8080 MHz	
Digital backend system (ADS-3000+)		
Analog IF input range	0–1.7 GHz	3 dB suppression level. Maximum number of IF input signals is 4.
Minimum time between recording intervals (scans)	0 second	System settings can be changed every seconds synchronized with 1 p/s signal
Output ports	Four VSI-H ports and two 10 GbE ports	Maximum output rate: - 4Gb/s/port (10 GbE ports) - 2Gb/s/port (VSI-H ports)
Subchannels (i.e., recordable channels)		
Digital down-conversion mode	Output bandwidth, max resolution, and max number of channels: – 32,16,8,4 MHz, 4 bit, 16 ch – 32,16,8,4 MHz, 8 bit, 8 ch	Each of four IF analog inputs can be selected for the input of each downconversion channel. Input IF signal shall be band-limited to 0–512 MHz, 512–1024 MHz, or 1024–1536 MHz in this mode.
Frequency resolution	1 Hz resolution (in the case of fixed frequency)	Fixed frequency or tuned to Doppler predicts
Sample format	In-phase and Quadrature-phase (I/Q) or Real sampling (USB/LSB)	

CCSDS REPORT CONCERNING DELTA-DOR—
TECHNICAL CHARACTERISTICS AND PERFORMANCE

Wide bandwidth output mode	Output bandwidth, resolution, and number of channels: – 2048 MHz, 2 bit, 2 ch – 1024 MHz, 4 bit, 2 ch – 512 MHz, 8 bit, 2 ch – 256 MHz, 8 bit, 2 ch – 128 MHz, 8 bit, 2 ch	No frequency tuning can be performed in this mode. Down-conversion is realized by bandpass filtering and decimation. Maximum number of IF analog inputs is limited to two in this mode.
Maximum allowed output rate	8192 Mbits/s	Number of subchannels, bandwidth, and resolution must be chosen to not violate this constraint

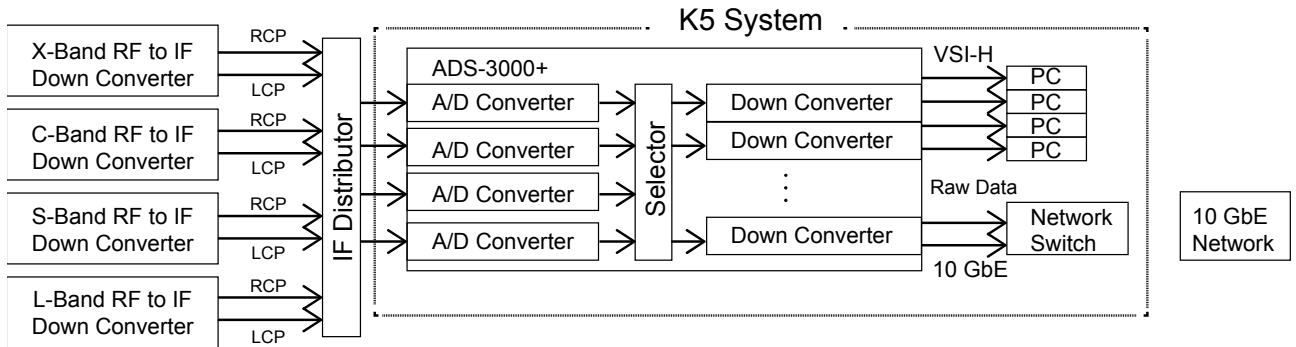


Figure 6-3: Simplified Block Diagram of Delta-DOR Back-End System in the JAXA Stations

ANNEX A

SPREAD SPECTRUM DOR CODE PARAMETERS

A1 INTRODUCTION

Subsection 3.2 presents the motivation for spread spectrum DOR tones as a method to reduce the phase dispersion error term. This annex presents informational background on the code selection, pulse shaping, and code parameters required to generate an appropriate spread spectrum signal. Then a set of recommended parameters is specified to optimize Delta-DOR performance.

A2 PN SPREAD SPECTRUM BACKGROUND

There are numerous options for generating PN sequences. One popular set of sequences is the set of maximum length sequences. These sequences have the property that the code length is $2^N - 1$, where N is the number of bits in the sequence. These codes have very good auto-correlation properties, but poor cross-correlation properties. For example, for maximum length sequences of length 8191 (13-bits) there are 730 unique sequences available, but at most, only a set of 4 sequences will share good cross-correlation properties. Since PN Delta-DOR may be used on clusters of cubesats in flight, it is desired to have more sequences available than this. Gold codes build upon maximum-length sequences for better cross-correlation properties. For example, for Gold Codes of length 8191, there is a set of 8193 sequences that have good cross-correlation properties. For this reason, it is recommended that Gold Codes be used for PN Delta-DOR.

CCSDS 415.1-B-1 (reference [32]) subsections 1.6.2 and 4.4 define LFSR and a representative Gold Code generator circuit. The same basic principles will be used in generating a Gold Code for PN DOR. However, PN DOR will require a circuit with more bits to create a longer sequence. The characteristic polynomials and initial seed of the generator circuit will change as well.

Determining the characteristic polynomials to use is fairly straightforward. The two LFSRs used to generate a Gold Code are each a maximum length sequence. The characteristic polynomial for a maximum length sequence must be a primitive polynomial. These primitive polynomials are well documented and well tabulated in literature. Then both of the maximum-length sequences selected must have cross-correlation values less than or equal to $\frac{N+2}{2}$, where N is the number of bits.

The number of bits in the LFSR is chosen so that the code period will satisfy the ambiguity resolution for spacecraft navigation. For cubesats or other missions with limited tracking data and unknown dynamics, it is conservative to have an ambiguity resolution of 1 millisecond. The number of bits in the LFSR sequence can then be computed from the ambiguity requirement, P , and the chiprate, R .

$$N = \log_2(PR + 1) \quad (34)$$

Since the number of bits in a LFSR must be an integer, the N must be rounded to the next largest integer. Also, since there are no Gold Code sequences when N is divisible by 4, the solution may again have to be rounded to the next largest integer until a Gold Code pair is found. There is no large penalty for using a larger code period than necessary.

Once the number of bits in the LFSR is known, the polynomial pairs can be selected, as noted above, by finding a pair of maximum-length sequences with good cross-correlation properties. Then a circuit similar to that in CCSDS 415.1-B-1 subsection 4.4 can be implemented to generate the sequence.

A3 PULSE SHAPING BACKGROUND

If the Gold Code sequence is transmitted as square pulses, the resulting spectrum will have a rounded shape in the frequency spectrum. This rounded spectrum does not closely resemble the flat quasar spectrum and will not reduce the phase dispersion error by a large factor. The spectrum can be flattened, however, by the use of a SRRC filter. The transfer function of a SRRC filter is listed in equation (35), below, and depends on both the chip rate, R , and the roll-off factor, β .

$$H(f) = \begin{cases} 1 & \text{for } \left(0 \leq |f| \leq \frac{R(1-\beta)}{2} \right) \\ \sqrt{\frac{1}{2} \left\{ 1 + \sin \left[\frac{\pi}{R\beta} \left(\frac{R}{2} - |f| \right) \right] \right\}} & \text{for } \left(\frac{R(1-\beta)}{2} \leq |f| \leq \frac{R(1+\beta)}{2} \right) \\ 0 & \text{for } \left(|f| > \frac{R(1+\beta)}{2} \right) \end{cases} \quad (35)$$

The frequency response for a variety of roll-off factors, β , is visualized in figure A-1, below. It is clear that a lower roll-off factor creates a flatter spectrum. But as the roll-off factor approaches zero, the filter is harder to implement in a digital transponder. So in practice, there is a limit to how low the roll-off factor can be.

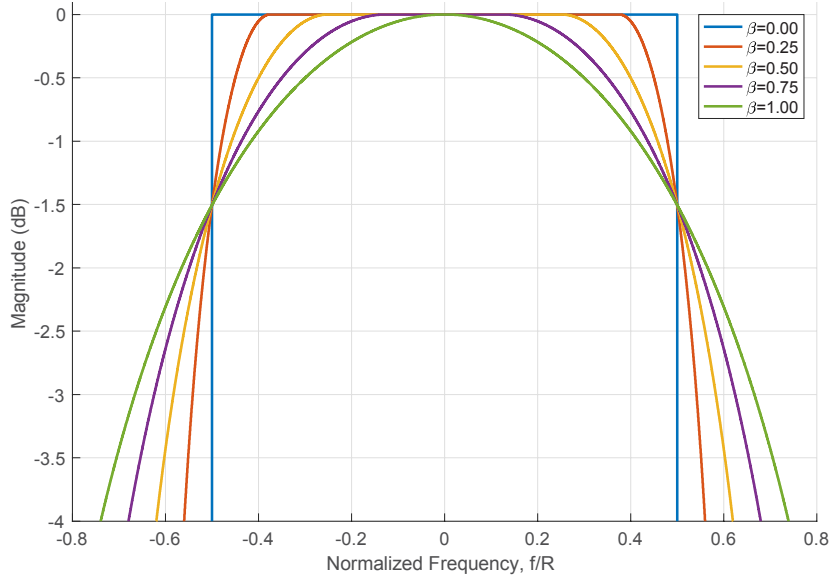


Figure A-1: SRRC Filter Response for a Variety of Roll-Off Factors

To have a spectrum that closely resembles the white-noise quasar signal, the frequency response should be within 1 dB of flat across at least 90 percent of the quasar channel bandwidth. This level of performance would result in a 90-percent reduction of the phase dispersion error. If the flatness of the transmitted spectrum is less than this, then the performance will also be reduced accordingly. It is possible to rearrange the SRRC frequency response equation to solve for what percentage of the desired spectrum is flat. This solution is in equations (36a) and (36b), where BW_{qsr} is the desired quasar channel bandwidth. Considering the expected flux at each band, the quasar channel bandwidth should be chosen wide enough so that thermal noise on the quasar measurement is not a dominant error. For X-band, the typical quasar channel bandwidth is 8 MHz, and for Ka-band, it is 32 MHz.

$$\%_{\text{flat}} = \frac{2R}{BW_{\text{qsr}}} \left(\frac{1}{2} - \frac{\beta}{\pi} \sin^{-1} \left[2(-1 \text{ dB})^2 - 1 \right] \right) \quad (36a)$$

$$\%_{\text{flat}} = \frac{2R}{BW_{\text{qsr}}} \left(\frac{1}{2} - \frac{\beta}{\pi} \sin^{-1} [0.262] \right) \quad (36b)$$

There is a trade-off between the chip rate and the roll-off factor that can provide a satisfactory level of flatness. This trade can be visualized in the contour plot of figure A-2. In this plot, the normalized chip rate is the chip rate divided by the desired quasar channel bandwidth (8 MHz for X-band and 32 MHz for Ka-Band). It should be noted that if $R(1 + \beta) > BW_{\text{qsr}}$, then some power will be wasted outside of the quasar bandwidth. The amount of power wasted is denoted by the red contour lines. The black contour lines denote what percentage of the spectrum is within 1 dB of flat. Any combinations where $R(1 + \beta) < BW_{\text{qsr}}$ were omitted since in those cases, the PN signal did not span the entire quasar bandwidth.

CCSDS REPORT CONCERNING DELTA-DOR—
TECHNICAL CHARACTERISTICS AND PERFORMANCE

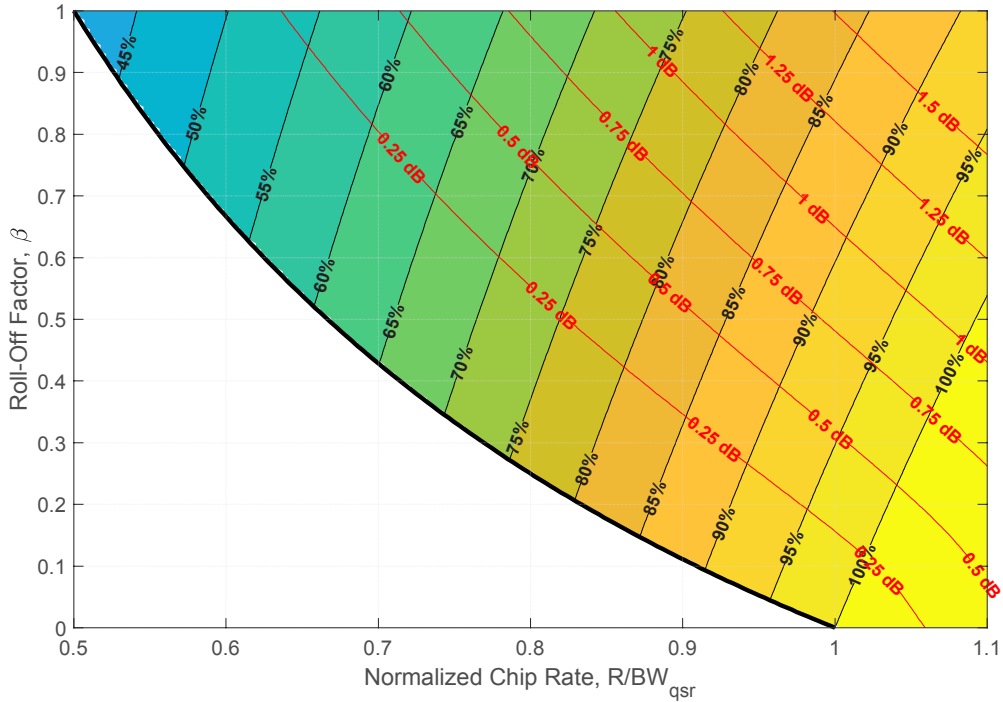


Figure A-2: Trade Between Chip Rate and Roll-Off Factor

Figure A-2, shows that there are many combinations that create a suitably flat spectrum, though some come at a cost of transmitting power outside the desired spectrum.

Any analog filters after the digital spectrum is generated can add further unwanted shaping to the spectrum. This is common in designs that include an analog Low Pass Filter (LPF) after a digital-to-analog converter. Figures A-3 and A-4 show the result of an LPF adding undesired shaping to the spectrum. It should be noted that there is roughly 3 dB of power variation across the 8 MHz PN spectrum, which should otherwise be flat.

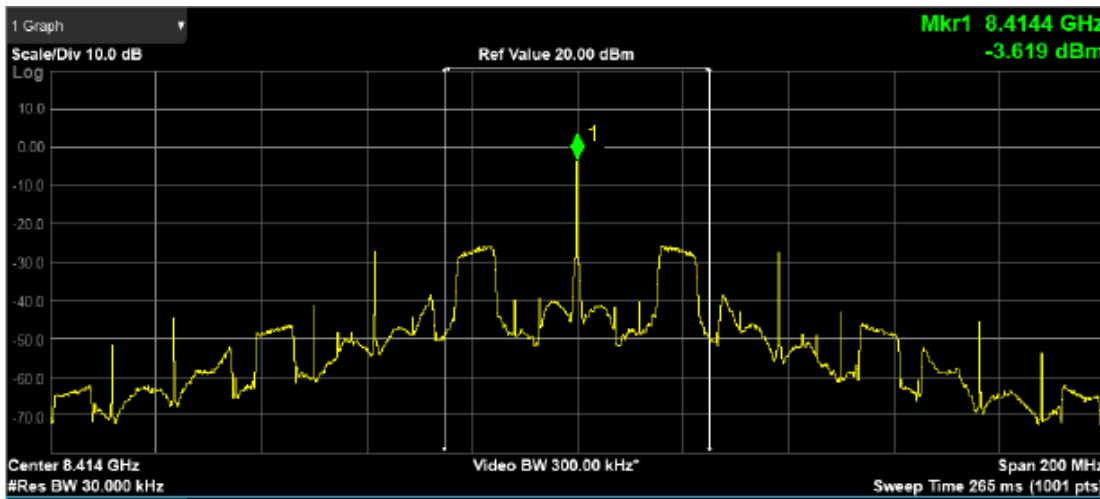


Figure A-3: PN Spectrum Shaping As a Result of an Analog LPF, 200 MHz Bandwidth

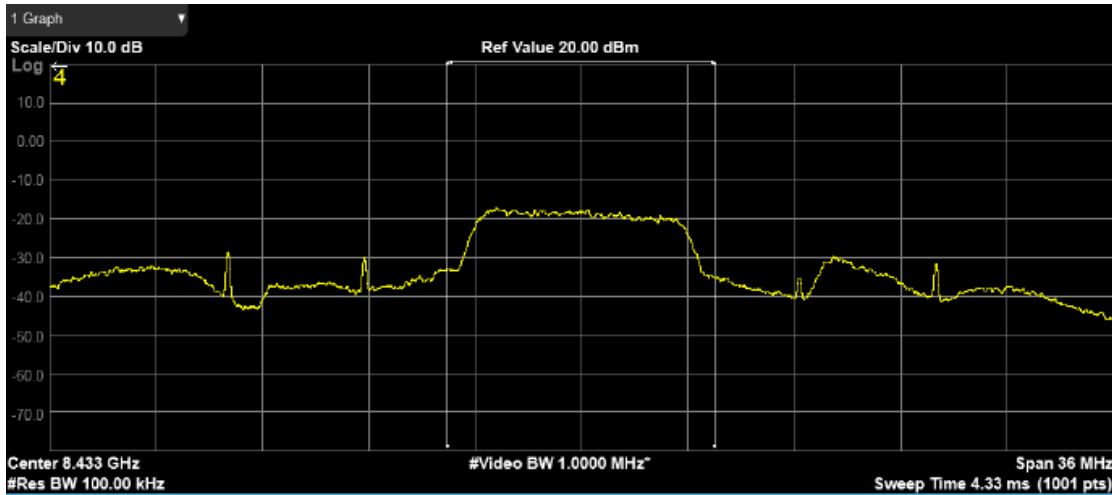


Figure A-4: PN Spectrum As a Result of an Analog LPF, 36 MHz Bandwidth

A corresponding equalization/pre-distortion filter can be designed to counteract this shaping. The design criterion is to create a flat power spectrum over the final output PN spectrum. Figure A-5 shows the same signal as figure A-4, but with an equalization/pre-distortion filter applied to remove the 3-dB power variation, leaving a flat spectrum.

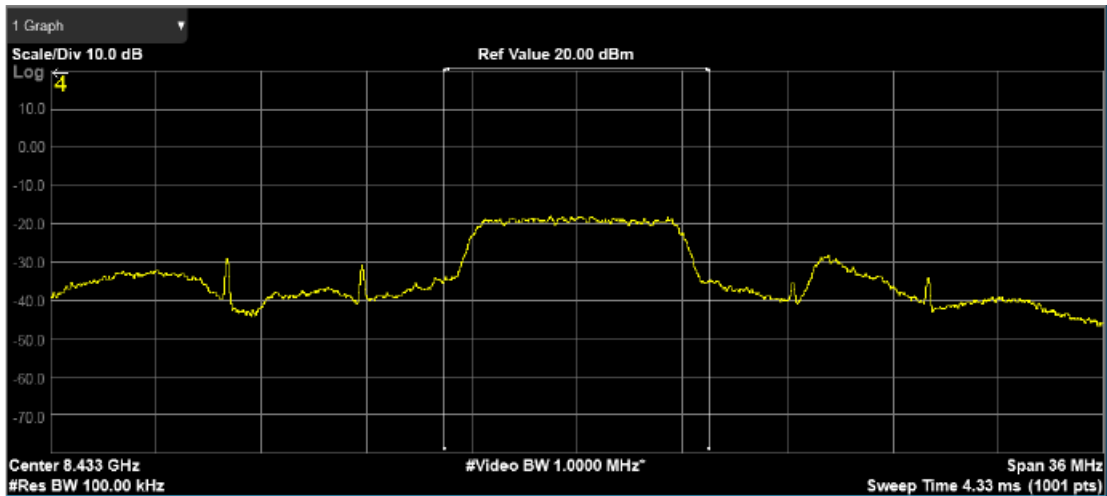


Figure A-5: PN Spectrum Flattened by Equalization/Pre-Distortion Filter, 36 MHz Bandwidth

For the best error reduction, the transmitted analog spectrum should be as flat as possible. This means that a digital pre-distortion filter is required for any cases in which analog filters add an unacceptable amount of shaping to the spectrum.

A4 RECOMMENDED PN CODE PARAMETERS

The recommended roll-off factor is 0.1. This creates a reasonably flat spectrum without an unreasonable amount of complexity in implementing the digital filter. At this roll-off factor, the chip rate must be 90% of the quasar bandwidth to have a spectrum in which 90 percent of the spectrum is within 1 dB of flat and none of the power is transmitted outside the quasar bandwidth. Since the quasar bandwidth is 8 MHz for X-band and 32 MHz for Ka-band, the recommended chip rate can be easily computed and is shown in table A-1, below.

Table A-1: Recommended Chip Rate and Roll-Off Factors

RF Band	Quasar Bandwidth	Chip Rate	Roll-Off Factor
X-Band	8 MHz	7.2 Mc/s	0.1
Ka-Band	32 MHz	28.8 Mc/s	0.1

With the chip rate known, the code length is then determined from equation (34), where the required ambiguity resolution is 1 millisecond. The recommended code length is shown in table A-2, below.

Table A-2: Recommended Code Length

RF Band	Chip Rate	N Bits	Code Length	Code Period
X-Band	7.2 Mc/s	13 bits	8191 chips	1.14 ms
Ka-Band	28.8 Mc/s	15 bits	32767 chips	1.14 ms

Finally, with the number of bits known, the polynomial pair for the Gold Code can be selected. This process is somewhat arbitrary since there are many combinations with the same performance, but all spacecraft need to use the same polynomials to prevent interference. The recommended polynomials are shown in table A-3, below. The initial LFSR seeds require inter-agency coordination for spacecraft that transmit on the same center frequency and might fall within the same antenna beam, in order to avoid potential interference.

Table A-3: Recommended Gold Code Polynomials

RF Band	1 st Polynomial	2 nd Polynomial
X-Band	$1 + x^9 + x^{10} + x^{12} + x^{13}$	$1 + x^3 + x^4 + x^6 + x^8 + x^9 + x^{13}$
Ka-Band	$1 + x^{14} + x^{15}$	$1 + x^3 + x^{12} + x^{14} + x^{15}$

These selected polynomials can be visualized by the corresponding generator circuits, below in figure A-6 and figure A-7. As previously mentioned, the initial seeds for Registers A and B will require inter-agency coordination and cannot broadly be defined *a priori*. In the figures below, this is represented by a series of asterisks (*). But in the final design, each register must be initialized with a defined initial seed that is a binary sequence of the same length as the register.

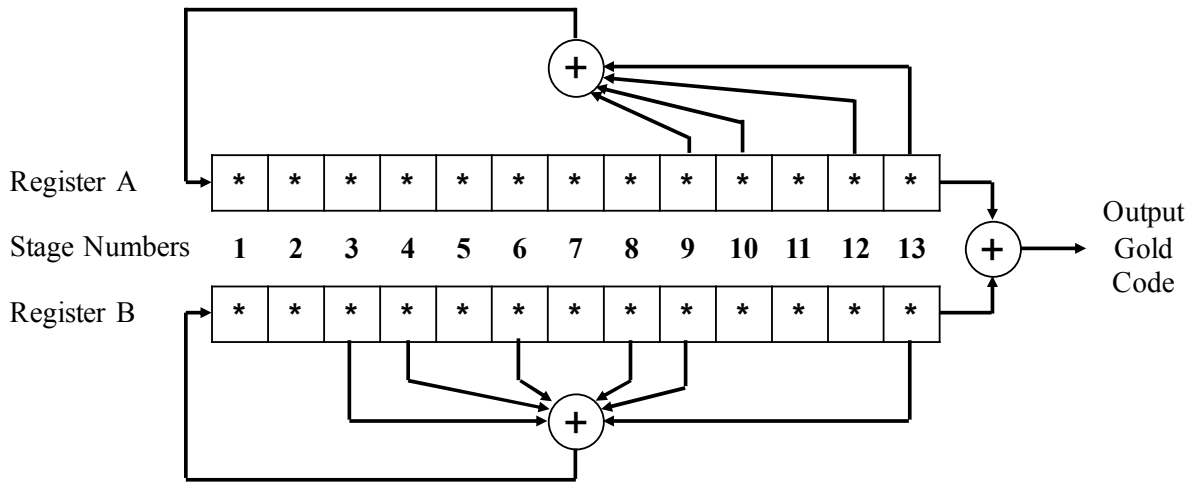


Figure A-6: Recommended X-Band Gold Code Generator Circuit

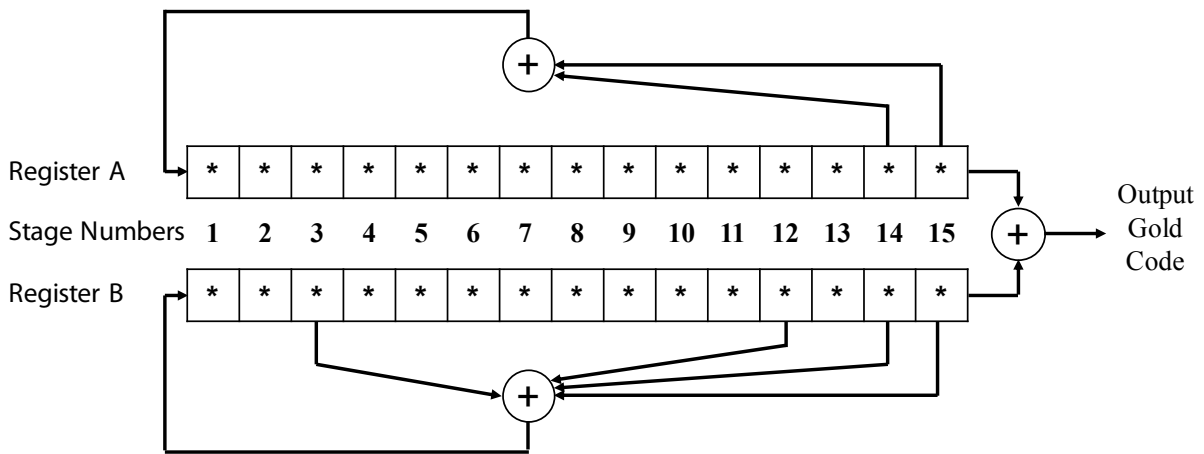


Figure A-7: Recommended Ka-Band Gold Code Generator Circuit

These recommended specifications are designed to provide the best Delta-DOR performance. Deviations from the recommended chip rate, roll-off factor, and code length may result in poorer performance, but may be acceptable, depending on a mission's needs. Deviations from the recommended polynomial pairs may result in interference with other spacecraft and will require advanced coordination between agencies.

For cross support between ground stations, the ground stations must be capable of recording the entire bandwidth (8 MHz for X-band and 32 MHz for Ka-band) of each frequency channel containing a spacecraft PN signal, just as is now done for the quasar signal. This change to the spacecraft signal improves Delta-DOR performance. However, the Raw Data Exchange Format (CCSDS 506.1-B-1, reference [33]) and the Recommended Practice for Delta-DOR Operations (CCSDS 506.0-M-2, reference [34]) do not change.

A5 SUMMARY

As presented in 3.2, implementation of spread spectrum Delta-DOR signals provides a few benefits. This annex presented the background information required to create suitable spread-spectrum signals and presented a standard set of parameters to optimize Delta-DOR performance.

ANNEX B

ABBREVIATIONS AND ACRONYMS

Δ DOR	Delta Differential One-way Ranging
AWVR	Advanced Water Vapor Radiometer
DC	downconversion
Delta-DOR	Delta Differential One-way Ranging
DOR	differential one-way ranging
DSN	Deep Space Network
ESOC	European Space Operations Centre
ESU	external storage unit
GNSS	Global Navigation Satellite System
GPS	Global Positioning System
IF	intermediate frequency
IFMS	intermediate frequency modem system
LCP	left-hand circular polarization
LFSR	linear feedback shift register
LNA	low noise amplifier
LO	local oscillator
LPF	low pass filter
LSB	lower sideband
OLR	Open Loop Receiver
PN	pseudo noise
RCP	right-hand circular polarization
RF	radio frequency
RSS	root sum square
SEA	Systems Engineering Area
SEP	Sun-Earth-probe
SFCG	Space Frequency Coordination Group
SNR	signal-to-noise ratio
SRRC	Square Root Raised Cosine
USB	upper sideband

CCSDS REPORT CONCERNING DELTA-DOR—
TECHNICAL CHARACTERISTICS AND PERFORMANCE

UT1	universal time number 1
UTC	Universal Time Coordinated
VLBI	very long baseline interferometry
VSI	VLBI standard interface
VSI-H	VLBI standard hardware interface
VSR	VLBI science receiver
WVSR	wideband VLBI science receiver